Journal of Mammalian Evolution (2026) 33:36
https://doi.org/10.1007/s10914-026-09828-0

RESEARCH

The distal humerus of *Pliobates cataloniae* (Primates: Pliopithecoidea): functional and locomotor inferences

Julia Arias-Martorell[1] · Ambra Figueroa-Torrejón[2] · Thomas A. Püschel[3] · Georgina Raventós-Izard[1] · Alessandro Urciuoli[1,4,5,6] · Jesús Gamarra[1] · Sergio Almécija[1,7,8,9] · David M. Alba[1]

Received: 9 February 2026 / Accepted: 22 June 2026

Abstract

The small-bodied stem catarrhine *Pliobates cataloniae* (Pliopithecoidea: Crouzeliidae), from the Miocene (11.6 Ma) of the Vallès-Penedès Basin (NE Iberian Peninsula), combines catarrhine symplesiomorphies and several crown hominoid-like features that are interpreted as convergent. The most obvious modern ape-like traits of *Pliobates* are found in the forelimb, particularly in the wrist and elbow joints. In the humerus, these include the lack of an entepicondylar foramen, a well-developed zona conoidea, and a globular capitulum. To quantitatively assess the degree of convergence between *Pliobates* and extant hominoids, we compare their distal humeral shape with a comparative sample including extant and extinct anthropoid primates. Shape is analyzed using landmark-based, 3D geometric morphometric techniques, while the locomotor repertoire of *Pliobates* and other extinct species is inferred using two-block partial least squares regression between shape and locomotor percentages. Our results indicate that the locomotor repertoire of *Pliobates* would have been dominated by orthograde behaviors such as climbing/clambering and suspension, in agreement with its ape-like humero-radial joint (which is functionally related to enhanced prono-supination). Nevertheless, the humeroulnar joint of *Pliobates* lacks the stabilization mechanisms that are characteristic of extant hominoids and necessary for frequently engaging in suspensory behaviors. We conclude that, while suspension was probably part of the locomotor repertoire of *Pliobates*, this taxon did not perform the acrobatic suspensory behaviors characteristic of the similarly-sized, extant hylobatids. Consequently, we interpret the ape-like humeroradial joint of *Pliobates* as an adaptation for climbing rather than modern ape-like suspensory behaviors.

Keywords Crouzeliidae · Functional morphology · Geometric morphometrics · Locomotion · Miocene · Prono-supination

Julia Arias-Martorell and Ambra Figueroa-Torrejón contributed equally to this work.

✉ Julia Arias-Martorell
julia.arias@icp.cat

✉ Ambra Figueroa-Torrejón
ambrafig@ucm.es

[1] Institut Català de Paleontologia Miquel Crusafont (ICP-CERCA), Universitat Autònoma de Barcelona, c/ Columnes s/n, Campus de la UAB, 08193 Cerdanyola del Vallès, Barcelona, Spain

[2] Physical Anthropology Unit, Department of Biodiversity, Ecology, and Evolution, Faculty of Biological Sciences, Universidad Complutense de Madrid, Madrid, Spain

[3] Institute of Human Sciences, School of Anthropology and Museum Ethnography, University of Oxford, Oxford, UK

[4] Department of Paleontology, University of Zurich, Zürich 8006, Switzerland

[5] Division of Palaeoanthropology, Senckenberg Research Institute and Natural History Museum Frankfurt, 60325 Frankfurt am Main, Germany

[6] Departamento de Ciencias de la Vida, Universidad de Alcalá, Cátedra de Otoacústica Evolutiva y Paleoantropología (HM Hospitales-UAH), Alcalá de Henares, Madrid 28871, Spain

[7] Institució Catalana de Recerca i Estudis Avançats (ICREA), Pg. Lluís Companys 23, Barcelona 08010, Spain

[8] Division of Anthropology, American Museum of Natural History (AMNH), New York, NY 10024, USA

[9] New York Consortium in Evolutionary Primatology, New York, NY 10024, USA

Published online: 17 July 2026

Introduction

Pliopithecoids constitute a clade of stem catarrhines from Eurasia that is first recorded in the Early Miocene of Asia (19–18 Ma; Harrison and Gu 1999; Begun 2002, 2017; Harrison 2013; Harrison et al. 2020). Among stem catarrhines, they are considered to be more derived than propliopithecoids from Afro-Arabia, but less so than some other extinct catarrhines from the Miocene of East Africa, such as dendropithecids (Andrews et al. 1996; Harrison 2005, 2013; Urciuoli et al. 2021, 2026; Bouchet et al. 2024b). Here we follow Bouchet et al. (2024b) in recognizing three pliopithecoids families (Dionysopithecidae, Pliopithecidae, and Crouzeliidae), with the last one subdivided into two subfamilies (Anapithecinae and Crouzeliinae)—see Harrison et al. (2020), and references therein, for an alternative systematic scheme. Pliopithecoids are mostly recorded by dentognathic remains and, hence, the three partial skeletons of the Middle Miocene pliopithecid *Epipliopithecus vindobonensis* (Zapfe and Hürzeler 1957; Zapfe 1958, 1961) were until recently the main reference for the postcranial body plan of the whole clade (e.g., Begun 2002; Harrison 2005, 2013). This situation recently changed with the discovery and analysis of the partial skeleton of the small-bodied catarrhine *Pliobates cataloniae* (Alba et al. 2015; Bouchet et al. 2021, 2024a, 2024b; Raventós-Izard et al. 2025). *Pliobates* is known from two roughly coeval localities (11.6 Ma) of the Abocador de Can Mata (ACM) macrosite (Alba et al. 2017, 2022), in the Vallès-Penedès Basin (NE Iberian Peninsula). Even though it was originally interpreted as a stem hominoid (Alba et al. 2015), it has been most recently reinterpreted as a crouzeliid pliopithecoid closely related to other, poorly-known small-bodied crouzeliines from Europe (Bouchet et al. 2024a, 2024b, 2025). Previous cladistic analyses had reached similar, but less detailed conclusions (Nengo et al. 2017; Gilbert et al. 2020a, 2020b; Ji et al. 2022), but the description of new diagnostic dental material by Bouchet et al. (2024a) conclusively show the possession of crouzeliid synapomorphies. The crouzeliine status of *Pliobates* was further confirmed by a cladistic analysis based on craniodental characters (Bouchet et al. 2024b, 2025), as well as morphometric comparisons of molar endostructural shape (Bouchet et al. 2024a, 2025). Accordingly, these authors concluded that the postcranial similarities with hominoids are homoplastic.

Based on the postcranial anatomy of *Epipliopithecus* (Zapfe 1958, 1961; Bacon 1994; Rein et al. 2011, 2015; Senut 2012; Arias-Martorell et al. 2015), pliopithecoids have been customarily characterized as retaining multiple plesiomorphic features relative to crown catarrhines, including, among others, the presence of an entepicondylar foramen in the distal humerus and a hinge-like carpometacarpal joint at the thumb (Szalay and Delson 1979; Harrison 1987, 2013; Andrews et al. 1996; Begun 2002, 2017; but see Alba and Moyà-Solà 2014). The locomotor repertoire of *Epipliopithecus* has been generally reconstructed as an arboreal quadruped with some degree of suspensory behaviors (Fleagle 1983; Rein et al. 2011, 2015; Harrison 2013; Arias-Martorell et al. 2015). The postcranial material available for *Pliopithecus* is much more restricted, overall being suggestive of semiterrestrial quadrupedalism and slow climbing abilities with no evidence of suspensory adaptations (Senut 2012; Alba and Moyà-Solà 2014; Arias-Martorell et al. 2015). Among anapithecines, the femora and phalanges of *Anapithecus* are indicative of a higher reliance on suspensory behaviors than in *Epipliopithecus* (Begun 1988, 1993; Kordos and Begun 1999, 2001). A proximal manual phalanx attributed to the anapithecine *Laccopithecus* (Meldrum and Pan 1988; Begun 2002; Harrison and Rein 2016: SOM fig. S2) was also interpreted as indicative of hylobatid-like suspensory behaviors, but was recently reinterpreted as more likely belonging to a sivaladapid (Harrison 2025). Finally, for crouzeliines, the proximal radius of *Barberapithecus* evinces better climbing abilities than in pliopithecids (Arias-Martorell et al. 2021), while the calcaneus and talus of *Crouzelia* have been interpreted as indicative of semiterrestrial quadrupedalism (Senut 2012). Overall, this evidence suggests that pliopithecoids exhibited a considerable diversity of locomotor behaviors, ranging from semiterrestrial quadrupedalism to arboreal quadrupedalism and climbing, and even some degree of suspensory behaviors (particularly in anapithecines; Arias-Martorell et al. 2015, 2021). The partial skeleton of *Pliobates*, however, most clearly suggests that this crouzeliine displayed a varied locomotor repertoire, given the combination of primitive (stem catarrhine-like) postcranial features with other, more derived (crown hominoid-like) ones (Alba et al. 2015; Bouchet et al. 2024b; Raventós-Izard et al. 2025). This mosaic of features is evident at the elbow joint, where evidence from the ulna (Raventós-Izard et al. 2025) and the radius (Arias-Martorell et al. 2026) shows that the humeroulnar articulation is much more plesiomorphic than the radioulnar one, which is in turn interpreted as convergent with that of crown hominoids (Bouchet et al. 2024b).

From a morphofunctional viewpoint, elbow and wrist shape indicate that the forearm of *Pliobates* displayed a wide pronation-supination range, compatible with slow above-branch quadrupedalism and cautious eclectic climbing with non-stereotypical postures—but not with hylobatid-like brachiation, despite the likely possession of a suspensory component in its locomotor repertoire (Alba et al. 2015; Raventós-Izard et al. 2025; Arias-Martorell et al. 2026). Given the convergences with crown hominoids, the combination of locomotor behaviors inferred for *Pliobates*—without a clear living analog—is potentially informative

about the emergence of orthograde behaviors during ape evolution (Bouchet et al. 2024b; Raventós-Izard et al. 2025; Arias-Martorell et al. 2026). This supports the likelihood of an early stage emphasizing cautious climbing (Cartmill and Milton 1977; Sarmiento 1995; Alba et al. 2015; Daver and Nakatsukasa 2015) that would have preceded the subsequent acquisition of specific suspensory adaptations in various lineages (e.g., Larson 1998; Moyà-Solà et al. 2004, 2005; Almécija et al. 2009; Alba 2012). Here we describe the partial humerus of *Pliobates* and compare it with that of extant and extinct anthropoids (with emphasis on other stem catarrhines and fossil apes) to better assess the degree of convergence with extant hominoids at the elbow joint. Besides qualitative comparisons, we perform a quantitative analysis of distal humeral shape using 3D geometric morphometrics. We also use the results of this analysis to estimate the locomotor repertoire of *Pliobates* based on a partial least squares regression between distal humeral shape and quantitative locomotor data extracted from the literature. Based on morphofunctional considerations, we discuss the implications of the distal humeral morphology of *Pliobates* for understanding locomotor diversity in extinct catarrhines and the emergence of modern ape-like locomotor behaviors.

Materials and methods

Studied and comparative sample

The studied material includes a partial left humerus (IPS58443.15; Fig. 1) that belongs to the holotype partial skeleton of *P. cataloniae*, recovered from locality ACM/C8-A4 (els Hostalets de Pierola, Catalonia, Spain) and attributed to a female individual (Alba et al. 2015). This specimen was only preliminarily reported by Alba et al. (2015: figs. 5A–D, 6A–D) and is first described in detail and analyzed here. It is housed in the Institut Català de Paleontologia Miquel Crusafont (ICP; Sabadell, Spain). The fossil was µCT-scanned at the facilities of the Centro Nacional de Investigación sobre la Evolución Humana (CENIEH; Burgos, Spain) with a high-resolution X-ray µCT scanner model Phoenix V|Tome|X s 240 (GE Sensing & Inspections Technologies). The µCT acquisition was carried out at 150 kV with a current of 125 µA, obtaining an isotropic voxel size of 24.9 µm. The X-ray beam was filtered by a 0.2 mm-thick copper absorber. A 3D high quality surface model was generated from the µCT scan using Avizo v. 6.3 (Thermo Fisher Scientific, Waltham, USA) and is openly available from the MorphoSource digital repository (https://doi.org/10.17602/M2/M768930).

The extant comparative sample includes 140 3D models from 15 anthropoid genera (Table 1) corresponding to 29 species (Online Resource 1: Table S1). In turn, the fossil comparative sample includes nine additional distal humeri of anthropoid primates, from propliopithecoids (*Aegyptopithecus*) and pliopithecoids (*Epipliopithecus*), to dendropithecids from East Africa (*Dendropithecus* and *Simiolus*), fossil cercopithecoids (*Microcolobus*) and atelids (*Caipora*), and both stem and crown hominoids (*Ekembo* and *Sivapithecus*, respectively; Table 2).

Three-dimensional models of right humeri from the comparative sample were mirrored using Avizo so they could be analyzed together with left humeri. The models obtained by the authors (Online Resource: Table S1), including those of fossils, were produced using a NextEngine surface laser scanner (NextEngine, Inc., Santa Monica, USA) and two different high-resolution µCT scanners (Online Resource 1: Table S1): an industrial µCT scanner ACTIS 225/300 (BIR, Inc., Lincolnshire, USA), located in the Department of Human Evolution, Max Planck Institute for Evolutionary Anthropology (Leipzig, Germany) and a µCT scanner Nikon XT 225 ST (Nikon Corporation, Tokyo, Japan), located in the Cambridge Biotomography Centre, Department of Zoology, University of Cambridge (UK). Samples scanned with the NextEngine laser scanner were obtained with a resolution of > 10,000 points per square inch; individuals were scanned in two or more positions (vertically and horizontally oriented) with 6 to 12 partitions and merged using ScanStudio HD PRO software v. 1.3.2 (NextEngine, Inc., Santa Monica, USA). The isotropic voxel size range for the µCT scan sample is 21.9–51.5 µm. 3D models produced with the laser scanner were processed (mesh irregularity cleaning, hole filling, among others) using Geomagic Wrap 2017 (3D Systems, Inc., Morrisville, USA) and Avizo software. The 3D models of fossil specimens were obtained from high quality casts housed at the ICP except in the case of KNM-RU2036 AK (*Ek. heseloni*) and KNM-RU 2097 (*D. macinnesi*), which were scanned from the original specimens by JAM at the National Museums of Kenya (KNM, Kenya) with a surface laser scanner. KNM-NA 47916 A was scanned also at the KNM with a structured light scanner by L. Pallas and shared with the authors with permission from M. Nakatsukasa. The CT scan of DPC 8702 (*Aegyptopithecus zeuxis*) was downloaded from MorphoSource (https://n2t.net/ark:/87602/m4/M37077) from the collections of the Duke Lemur Center Museum of Natural History. Details of the type of scanner used for the extant sample obtained from MorphoSource can be found in Online Resource 1: Table S1, in MorphoSource, and, when indicated, in Almécija et al. (2024).

Fig. 1 Left partial humerus (IPS58443.15) of *Pliobates cataloniae* in posterior (**a**), lateral (**b**), anterior (**c**), medial (**d**), and distal (**e**) views. Scale bar equals to 2 cm

Geometric morphometric analyses

The shape affinities of the distal humerus of *P. cataloniae* were evaluated using a protocol of 30 landmarks (Table 3; Fig. 2). The specimen is missing part of the most anterior point of the medial margin of the trochlea (Fig. 1), so that the protocol was designed to capture the preserved areas (i.e., no landmarks were placed on the parts of the trochlea damaged in *Pliobates*). Both type I and II landmarks (i.e., homologous landmarks as defined in Bookstein 1991 and O'Higgins 2000) were used to better capture the local features of the distal humerus. Some of the landmarks included in the protocol were used in previous research, such as those distributed along the lateral edge of the capitulum, at the projections of the epicondyles, and at the deepest point of the olecranon fossa and in its surroundings (Bacon 2000; Halenar 2011). Additional landmarks were added to the entire trochlea, to capture its depth and margins, because they are characteristic aspects that differentiate hominids from platyrrhines, cercopithecoids, and fossil catarrhines

Table 1 Extant primate comparative sample used in this study. See abbreviations in the main text

Genus	*n*	Sex (F/M/?)	Side (L/R)	Repositories
Alouatta	10	2/2/6	4/6	AMNH, USNM, ZMB, ZMS, MS
Ateles	18	2/2/14	8/10	AMNH, USNM, ZMB, MS
Cebus	6	2/2/2	4/2	AMNH, USNM, MS
Colobus	5	2/3/0	5/0	AMNH, USNM
Gorilla	22	7/4/11	13/9	AMNH, USNM, RMCA, PC, CMNH, MS
Hoolock	2	1/1/0	2/0	AMNH
Hylobates	4	2/2/0	2/2	AMNH, NMNH
Lagothrix	2	0/0/2	0/2	USNM, MS
Macaca	6	2/2/2	4/2	AMNH, USNM, ZMB
Nasalis	3	2/1/0	2/1	AMNH, USNM
Nomascus	3	1/2/0	3/0	AMNH, NMNH
Pan	24	7/5/12	17/7	AMNH, USNM, RMCA, SBU, MPI, YPM, MS
Papio	6	2/2/2	4/2	AMNH, USNM, ZMB
Pongo	21	5/6/10	13/8	AMNH, USNM, MS
Symphalangus	8	1/2/5	4/4	AMNH, ZMB, NMNH, UWBM, MS

(McHenry and Corruccini 1975). Landmarks were also added to the supracondylar crest because of its known relationship with locomotor muscle development and its variation among species (DeSilva et al. 2013; Monroy-Cendales et al. 2020).

All statistical analyses were performed in R v. 4.2.2 (R Core Team 2021). We used generalized Procrustes analysis (GPA) to translate, rotate, and scale to unit centroid size (CS) landmarks coordinates using the Morpho v. 2.10 package (Schlager et al. 2022). Missing landmarks in the slightly damaged *Aegyptopithecus* humerus DPC 8702—specifically, L6 in the trochlea and L22 in the capitulum (Table 3; Fig. 2)—were estimated using the function *estimate.missing* in the Geomorph v. 4.0.4 package (Adams et al. 2022). We applied the thin-plate spline approach, as it provides more robust estimates for fossil specimens and reduces the risk of overfitting in studies with relatively small sample sizes (Gunz et al. 2009). A between-group principal component analysis (bgPCA; Mitteroecker and Bookstein 2011) was performed on the GPA-transformed coordinates of the extant anthropoid sample, using major clades (platyrrhines, cercopithecines, colobines, hylobatids, and hominoids) as a grouping factor to identify the main patterns of shape variation in the sample. The fossil specimens were projected a posteriori onto the morphospace generated by the bgPCA and the bgPCs that accounted for more than 5% of the variance were kept for subsequent analyses. Bivariate scatter plots between bgPCs were performed to assess group distribution, as well as to visualize shape changes along each bgPC. Shape configurations at the extremes of each bgPC were warped onto the distal humerus of an individual of the extant sample identified as the closest to the mean configuration of the morphospace using the function *findmeanspec* in Geomorph.

A cross-validated bgPCA was computed to compare its results with those of the bgPCA and with raw shape coordinates, to rule out potentially spurious grouping structure (Bookstein 2019; Cardini and Polly 2020). Differences

Table 2 Fossil sample used in this study

Catalogue No.	Species (family)	Site (country)	References
IPS58443.15	*Pliobates cataloniae* (Crouzeliidae)	Abocador de Can Mata (Spain)	Alba et al. (2015: figs. 5A -E, 6A)
DPC 8702	*Aegyptopithecus zeuxis* (Propliopithecidae)	Fayum (Egypt)	Johnes (2004: table M-2)*
Individual II (NHMW 1970/1397/0003)	*Epipliopithecus vindobonensis* (Pliopithecidae)	Devínska Nová Ves (Slovakia)	Zapfe (1958: pl. 1 A, 1961: fig. 51)
KNM-RU 2097	*Dendropithecus macinnesi* (Dendropithecidae)	Rusinga Island (Kenya)	Le Gros Clark and Thomas (1951: pl. 4 fig. 8), Andrews and Simons (1977: fig. 3B), Senut (1989: pl. IX), Rose et al. (1992: fig. 4D)
KNM-MO 17022 A	*Simiolus enjiessi* (Dendropithecidae)	Moruorot (Kenya)	Rose et al. (1992: fig. 5); Rose (1997), Rossie et al. (2012)
KNM-WK 17009 A	*Simiolus enjiessi* (Dendropithecidae)	Kalodirr (Kenya)	Leakey and Leakey (1987: fig. 3); Rose et al. (1992: fig. 1)
KNM-NA 47916 A	*Microcolobus* sp. (Cercopithecidae)	Nakali (Kenya)	Nakatsukasa et al. (2010: fig. 4b,d,f)
KNM-RU 2036 AK	*Ekembo heseloni* (Proconsulidae)	Rusinga Island (Kenya)	Napier and Davis (1959: figs. 7a, 8a, 9a, pl. 3 figs. 12 -14, pl. 4 figs. 16, 17); Senut (1989: pl. VI)
GSP 30730	*Sivapithecus indicus* (Hominidae)	Potwar Plateau (Pakistan)	Pilbeam et al. (1990: figs. 1F, 2F); Kelley (2002: fig. 21.5A–B)
IGC-UFMG605	*Caipora bambuiorum* (Atelidae)	Toca da Boa Vista (Brazil)	Cartelle and Hartwig (1996: fig. 5A); Aristide et al. (2019)

*DPC 8702 has not been formally described but is here assigned to the propliopithecoid (stem catarrhine) *Aegyptopithecus zeuxis*, as catalogued on its digital source (https://n2t.net/ark:/87602/m4/M37077)

Table 3 Landmark protocol used in this study. The landmarks are all type I or II (Bookstein 1991; O'Higgins 2000)

Landmark No.	Description
Epicondyle	
L1	Most lateral point on the lateral epicondyle
L2	Medial projection of the medial epicondyle
L3	Posterior point on the lateral epicondyle
Trochlea	
L4	Proximomedial extreme of the trochlea (posterior)
L5	Most distal point on the medial margin of the trochlea
L6	Proximomedial extreme of the trochlea (anterior)
L7	Proximal extreme on the posterior surface of the trochlear groove
L8	Distal extreme of the trochlear groove
L9	Most anterior point on the trochlear groove
L10	Proximal extreme on the anterior surface of the trochlear groove
L11	Proximolateral extreme of the trochlea (posterior)
L12	Most distal point on the lateral margin of the trochlea
L13	Most anterior point on the lateral margin of the trochlea
L14	Proximolateral extreme of the trochlea (anterior)
Conoid zone	
L15	Most distal point on the conoid zone
L16	Most anterior point on the conoid zone
L17	Superior margin of the conoid zone
Capitulum	
L18	Posteroinferior margin of the capitulum
L19	Most anteriorly protruding point on the capitulum
L20	Superior margin of the capitulum
L21	Distolateral margin of the capitulum
L22	Lateral margin of the capitulum
L23	Proximolateral margin of the capitulum
Olecranon fossa	
L24	Deepest point within the olecranon fossa
L25	Most lateral point on the lateral margin of the olecranon fossa
L26	Most medial point on the medial margin of the olecranon fossa
L27	Most proximal point on the proximal margin of the olecranon fossa
Supracondylar crest	
L28	Point of inflection just proximal to the lateral epicondyle, on supracondylar crest
L29	Point of inflection just proximal to the medial epicondyle, on the supracondylar crest
L30	Deepest point in excavation of the outer medial trochlea (posterolateral to the groove for the ulnar nerve)

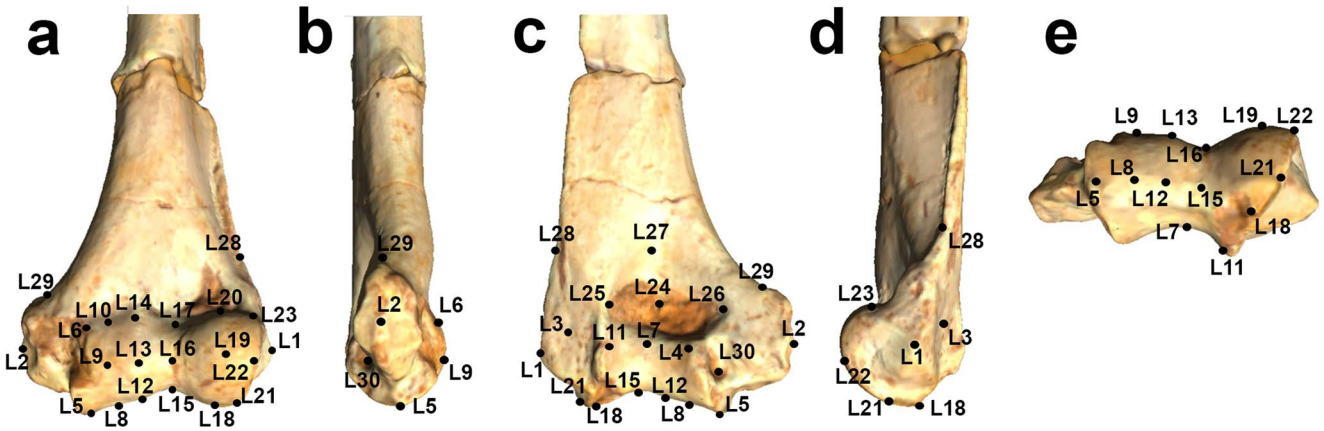

Fig. 2 Landmark protocol used in this study, illustrated on a 3D model of the left distal humerus fragment of *Pliobates cataloniae* (IPS58443.15), in anterior (**a**), medial (**b**), posterior (**c**), lateral (**d**), and distal (**e**) views. A description of the landmarks (L) can be found in Table 3

among group means were then tested by means of a permutational analysis of variance (PERMANOVA), based on Euclidean distances between the means (1000 permutations). In particular, the Z scores and R^2 for group differences were computed in the shape data, the bgPCA, and the cross-validated bgPCA using the RRPP package v. 1.2.3 for R (Collyer and Adams 2022). To assess the affinities of each fossil specimen with the a priori defined groups, we computed their typicality probabilities using the function *typprobClass* in Morpho based on the bgPCA.

To assess potential allometric effects, the correlation between bgPC scores (accounting for >5% variance) and log-transformed (with natural logarithms) centroid size (ln CS) was assessed through phylogenetic generalized least squares (PGLS) regression (Grafen 1989; Adams 2014) using Geomorph. This methodology modifies linear regression to explore the relationship between predictor and response variables while accounting for the non-independence of species data due to shared ancestry, by incorporating the expected covariance structure derived from a phylogenetic tree (Symonds and Blomberg 2014). The PGLS regressions were computed based on a time-calibrated phylogenetic tree (Online Resource 1: Fig. S1a) downloaded from the 10kTrees v. 3 website for extant taxa (Arnold et al. 2010; https://10ktrees.nunn-lab.org/). Using the same phylogenetic tree, the phylogenetic signal embedded in the shape of the distal humerus among extant anthropoids was computed using Blomberg's K (Blomberg et al. 2003) statistic. Blomberg's K was calculated for the bgPCs accounting for >5% of variance as well as the landmark configurations after GPA (landmark configurations) using Phytools v. 1.0–3 package (Revell 2022) in R: it tests the null hypothesis of no phylogenetic signal (that closely related species do not resemble each other more than distant species do) by comparing the distribution of the observed data with the distribution expected under a Brownian motion (BM) model of evolution (Blomberg et al. 2003; Kamilar and Cooper 2013). $K=0$ implies a model of evolution that closely resembles that expected under BM; for $K<1$, the variance accumulates within the clades, and closely related taxa resemble each other less than expected, signaling independent evolution (i.e., homoplasy); finally, when $K>1$, taxa (particularly non-closely related taxa) are more similar than expected under a BM model of evolution, implying that the variance accumulates among clades (e.g., as the result of stabilizing selection). Additionally, we calculated the phylogenetic signal of the sample, including the fossils, to observe the differences in signal between the two sets of tests. Extinct species were added to the phylogenetic tree (Online Resource 1: Fig. S1b) based on their phylogenetic relationships, as inferred by recent cladistic analyses and reviews (Gilbert et al. 2020b: fig. 4; Pugh 2022: fig. 5; Urciuoli and Alba 2023; Bouchet et al. 2024b: fig. 5). Their divergence times were arbitrarily set 1 Ma before the estimated divergence age of the next derived node (e.g., Almécija et al. 2013). Tip age estimates for the fossils were as follows: *Caipora bambuiorum*, 0.1 Ma (faunal correlation age of the site Toca da Boa Vista; Cartelle and Hartwig 1996); *Epipliopithecus vindobonensis*, 14.15 Ma (average of the maximum and minimum age ranges for MN6 in central Europe; van der Meulen et al. 2011); *Simiolus enjiessi*, 17.2 Ma (average of the ages of Kalodirr [16.7 Ma] and Moruorot [17.7 Ma]; Rose et al. 1992); *Dendropithecus macinnesi*, 17.8 Ma (age of locality R3a from the Hiwegi Formation of Rusinga Island; Drake et al. 1988; Senut 1989; Peppe et al. 2009); *Ekembo heseloni*, 17.8 Ma (age of the Kulu Formation of Rusinga Island; Peppe et al. 2009); *Sivapithecus indicus*, 10.8 Ma (age of the locality Y67 in the Chinji Formation; Pilbeam et al. 1990); *Aegyptopithecus zeuxis*, 30.2–29.2 Ma (age of quarries I and M from the Jebel Qatrani Formation; Seiffert 2006); and *Microcolobus* sp. 9.8–9.9 Ma (age of the Nakali Formation; Nakatsukasa et al. 2010).

Locomotor repertoire analysis

Previous studies indicated that it is possible to distinguish between main locomotor modes and substrate preferences using the shape of postcranial bones, as well as using this information to infer the locomotor behavior of fossil primates (e.g., Manfreda et al., 2006; Püschel et al. 2018, 2020). Many of these studies discretized locomotor categories or substrate preferences into a limited number of classes to enable the application of different classification algorithms. Although certainly valuable, these approaches have limitations that arise from the fact that any classification scheme is a simplification of the actual behavior observed in animals, as a result of shoehorning their diverse locomotor repertoires into a limited number of categories. As an alternative to overcome this limitation, other studies have applied two-block partial least squares analysis (2B-PLS) to assess the major patterns of covariation between a given shape data matrix (e.g., humeral shape) and a locomotor behavior data matrix (e.g., Almécija et al. 2015; Püschel et al. 2017). These studies have shown that it is possible to find strong covariation patterns between shape and locomotor data, thus indicating that the shape of certain skeletal elements can be potentially used to infer locomotor and postural behaviors. However, these works only focused on extant species and did not try to infer the locomotor repertoire of extinct species based on their fossil remains. In addition, the standard version of the 2B-PLS analysis in the morphometric literature corresponds to a symmetric analysis that, in its classic formulation, does not allow

the prediction of new data (Zelditch et al. 2012). There is, however, a type of analysis more comparable to regression, known as PLS-regression (PLSR), which permits the generation of predictive models (Wold et al. 2001). Some recent studies have successfully applied such an approach to infer the locomotor repertoire (i.e., the percentage of locomotor behaviors) in fossil primate taxa (e.g., Monclús-Gonzalo et al. 2023, 2025a, 2025b). Therefore, here we applied a PLSR approach to infer the locomotor repertoire of *Pliobates.*

The blocks of data consisted of: (1) distal humeral shape averaged by species; and (2) locomotor mode percentages (LMPs; i.e., the percentage time a species spends performing a certain type of locomotor behavior). A dataset of LMPs for the 32 extant species in the comparative sample was compiled from the literature (Online Resource 1: Table S2). Five different locomotor modes were considered, which were extracted from the standardized descriptions of Hunt et al. (1996) and have been used previously (sometimes with minor modifications) in other studies (Püschel et al. 2018, 2020; Monclús-Gonzalo et al. 2023, 2025a, 2025b; Raventós-Izard et al. 2025; Arias-Martorell et al. 2026): quadrupedalism (QWR), which includes the locomotor modes arboreal quadrupedal walking, bounding, and running; climbing (CL), which includes climbing, clambering, and vertical climbing (CL); leaping (L), including leaping, dropping, and hopping; and forelimb-dominated suspension (S), which includes bridging, brachiation (including ricochetal brachiation), and other types of suspensory locomotion (such as arm-swinging and non-acrobatic brachiation). Because the LMPs came from different literature sources, and not all behaviors reported in the original studies were considered, we rounded the LMPs to ensure that they add up to 100% for each species. In addition, to ensure that our locomotor estimates were between 0 and 100%, we first converted the percentages to proportions by dividing the percentages by 100, and then we applied a logit transformation to the resulting LMP proportion. The logit transformation of proportion data can be defined as ln (p / 1 – p), where p is a proportion. This transformation was done prior to carrying out the PLSR to avoid nonsensical results (e.g., LMPs higher than 100% or lower than 0%; e.g., Rein et al. 2011). Since ln (0) is undefined, we added 0.1% to any LMP value equal to zero and then we rounded up again the LMPs to ensure again that they added up to 100% before carrying out the logit transformation.

The PLSR is based on the same basic machinery as the standard 2B-PLS, which means that it finds latent variables that maximize covariation between two sets of variables by means of decomposing the covariance matrix of the two blocks into two sets of eigenvectors (one for each set of variables) and eigenvalues, using a singular value decomposition to generate a matrix of singular values (the square-roots of the eigenvalues), a matrix of eigenvectors for the first set of variables and the transpose of the matrix of eigenvectors for the second set of variables (Rohlf and Corti 2000). We carried out this step by using the *two.b.pls* function of the Geomorph package, and we ran 9999 iterations for significance testing. Then, instead of regressing the first block of variables (i.e., LMPs) on the second (i.e., distal humeral shape), the PLSR works by regressing the first block of variables on the vector obtained from the scores for the second block of variables (i.e., the LMPs were regressed on the distal humeral shape values that were projected onto the obtained singular vectors). This step was done using the *procD.lm* function of the same package (9999 iterations were used). To obtain LMP predictions, the distal humeral shape values were projected onto the obtained singular vectors and then multiplied by a matrix consisting of the linear model coefficients. This process was done with the humeral shape data of *Pliobates* and other extinct species to infer their locomotor repertoire. Since, prior to the PLSR, the LMPs were subjected to a logit transformation, the obtained predictions were transformed back into percentages by applying an inverse logit transformation defined as: $f(x)=\exp(x)/(1+\exp(x))$, where x corresponds to a logit transformed value. The predictions obtained were then rounded up again to ensure that they added to 100%. To assess the PLSR predictive performance, we performed a leave-one-out cross-validation (LOOCV), which means that separate analyses were carried out for each one of the predictions excluding the individual for which the prediction was being calculated (Kuhn and Johnson 2013). Using these cross-validated results, we computed the mean absolute error (MAE; i.e., the arithmetic average of the absolute errors) for the overall analysis and for each locomotor type, as well as the MAE per each species in the analyses, and per each locomotor behavior, to assess our prediction results using the extant sample (Willmott and Matsuura 2005).

Abbreviations

Institutional abbreviations: AMNH, American Museum of Natural History, New York, USA; **CENIEH**, Centro Nacional de Investigación sobre la Evolución Humana, Burgos, Spain; **CMNH**, Cleveland Museum of Natural History, Cleveland, USA; **DPC**, Duke Primate Center, Durham, USA; **GSP**, Geological Survey of Pakistan, Baluchistan, Pakistan; **IGC-UFMG**, Instituto Geociências Universidade Federal de Minas Gerais, Belo Horizonte, Brazil; **ICP**, Institut Català de Paleontologia Miquel Crusafont, Sabadell, Spain; **IPS**, acronym of the collections of the ICP (formerly, Institut de Paleontologia de Sabadell); **KNM**, National Museums of Kenya, Nairobi, Kenya; **MPI**, Max Planck Institute for Evolutionary Anthropology, Leipzig, Germany;

NHMW, Naturhistorisches Museum Wien, Vienna, Austria; **PC**, Powell-Cotton Museum, Birchington, UK; **RMCA**, Royal Museum for Central Africa, Tervuren, Belgium; **SBU**, Stony Brook University, New York, USA; **USNM/NMNH**, Smithsonian National Museum of Natural History, Washington D.C., USA; **ZMB**, Museum für Naturkunde - Leibniz Institute for Evolution and Biodiversity Science, Berlin, Germany; **ZMS**, Zoologische Staatssammlung Munchen, Munich, Germany; **UWBM**, University of Washington Burke Museum, Washington D.C., USA; **YPM**, Yale Peabody Museum, New Haven, USA. **Other abbreviations: bgPC**, between-group principal component; **bgPCA**, between-group principal component analysis; **BI**, bipedal walking; **CL**, clambering and vertical climbing; **CS**, centroid size; **F**, female; **GPA**, generalized Procrustes analysis; **L**, leaping, dropping, and hopping; **Le**, left; **LMP**, locomotor mode percentages; **LOOCV**, leave-one-out cross-validation; **M**, male; **MAE**, mean absolute error; **MS**, MorphoSource; **PERMANOVA**, permutational analysis of variance; **PGLS**, phylogenetic generalized least squares; **PLSR**, partial least squares regression; **QWR**, arboreal quadrupedal walking, bounding, and running; **Ri**, right; **r-PLS**, correlation coefficient from 2-block partial least squares analysis; **S**, bridging, brachiation, and suspensory locomotion; **µCT**, microcomputed tomography; **2B-PLS**, two-block partial least squares analysis; **?**, unknown sex.

Results

Description

The partial left humerus IPS58443.15 (Figs. 1 and 3a) measures 15.2 cm in total length (see additional measurements in Table 4). The humerus is preserved in three loosely fitting pieces and it is nearly complete, only lacking the humeral head. The distal epiphysis is broken above the medial and lateral supracondylar ridges, and the shaft is broken into two additional fragments, at approximately one third of the length proximally. The distal humeral fragment is well preserved except for two areas that show slight abrasion: the anterior part of the medial margin of the trochlea and the posteroinferior margin of the zona conoidea, behind the posteroinferior and distolateral margin of the capitulum. Both shaft fragments exhibit additional minor transverse cracks (Fig. 1).

The shaft is anteriorly straight and somewhat proximally retroflexed; it is round in cross section and becomes somewhat subtriangular proximally as there is a well-defined and flat deltoid insertion with a gracile deltoid crest; both the shaft and the humerus more broadly are relatively gracile overall. At the distal articular surface, the trochlea does not protrude distally; it is flat and lacks a trochlear groove. The medial keel is poorly developed and does not distally protrude significantly, while the lateral keel is only slightly distally protruding, which makes the overall trochlea not spool-shaped. The zona conoidea is well developed, with a moderately globular capitulum that does not expand posterolaterally and does not exhibit a capitular tail. There is no entepicondylar foramen. The radial fossa is deep and expanded both proximodistally and lateromedially. In contrast, the coronoid fossa is shallow, separated from the radial fossa by a slightly prominent ridge and with a slightly marked ulnar groove on its medial aspect. The medial epicondyle is proximodistally long and anteroposteriorly deep, while the lateral epicondyle is small and protrudes slightly laterally, being nearly aligned with the midpoint of the capitulum along the proximodistal axis. The most proximal end of the olecranon fossa is not clearly visible, and the proximal margin is not well defined. Nevertheless, the preserved portion does show a shallow fossa with no extension of the articular surface onto it.

Qualitative comparisons

The humeral shaft of *Pliobates* (Fig. 1) resembles that of cebids (Senut 1986; Rose 1994; McCrossin et al. 1998; Harrison 2010), as well as *Pliopithecus*, *Epipliopithecus* (Rose 1993a, 1994, 1997; Arias-Martorell et al. 2015), and *Dryopithecus* (from Saint-Gaudens; Lartet 1856; Pilbeam and Simons 1971; Begun 2009; Alba et al. 2011) in terms of slenderness, displaying a rounded cross section and a slight proximal retroflexion, while being anteriorly straight. It is also similar in the minimal shaft medial concavity to *Sivapithecus indicus* (Pilbeam et al. 1990: figs 1, 2), while being quite different from that of *Aegyptopithecus* (Fleagle and Simons, 1982; Gebo 1993)—which is overall quite robust—*Microcolobus* and *Dendropithecus*, all with anteroposteriorly compressed shafts (particularly at the distal end for the latter; Fig. 3b,d,i; Rose 1994, 1997; Harrison 2010, 2013; Nakatsukasa et al. 2010). The anteriorly straight shaft of *Pliobates* also differs from the condition exhibited by the latter fossil taxa, which display a marked concavity of the shaft in anterior view. It also differs from those of hominoids, atelids, and *Caipora* (Fig. 3g–h, m–n; Cartelle and Hartwig 1996; Alba et al. 2011), all of which display relatively straight to somewhat anteroflexed shafts. The slight shaft retroflexion of *Pliobates* differs from the condition of *Si. indicus*, in which retroflexion is seemingly absent (Moyà-Solà and Köhler 1996; Köhler et al. 2001; Alba et al. 2011)—although the shaft is crushed and retroflexion in the *Si. indicus* GSP 30730 specimen is thus difficult to ascertain (Richmond and Whalen 2001). The humeral shaft of *Pliobates* (and *Si. indicus*) is also quite different from that

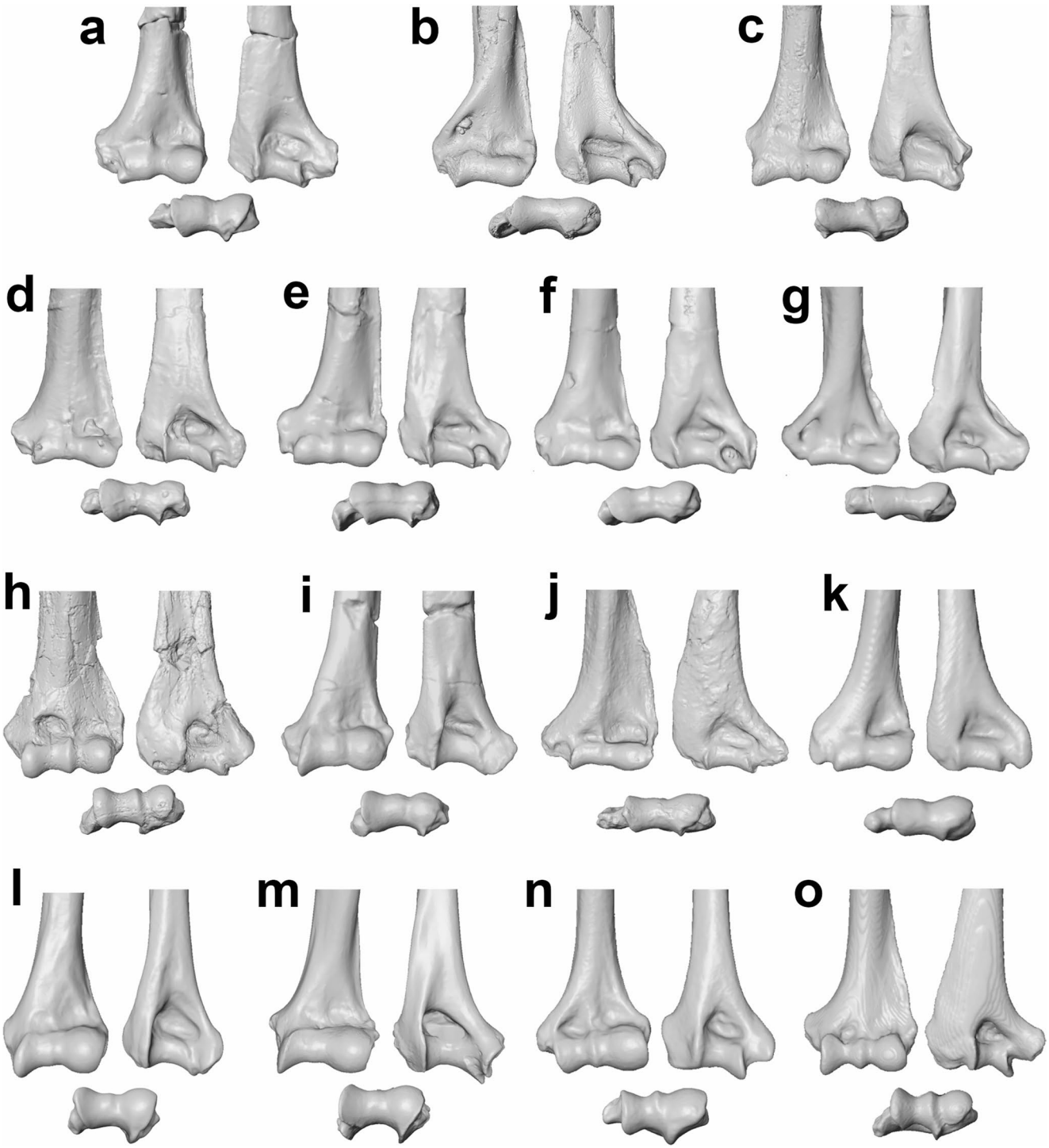

Fig. 3 Left distal humerus of *Pliobates cataloniae* compared with selected fossil and extant anthropoids in anterior (top left), posterior (top right), and distal (bottom) views: **a**. *P. cataloniae*, IPS58443.15; **b**. *Aegyptopithecus zeuxis*, DPC 8702; **c**. *Ekembo heseloni*, KNM-RU 2036 AK; **d**. *Dendropithecus macinnesi*, KNM-RU 2097; **e**. *Simiolus enjiessi*, KNM-MO 17022 A; **f**. *S. enjiessi*, KNM-WK 17009 A; **g**. *Epipliopithecus vindobonensis*, NHMW 1970/1397/0003 (Individual II); **h**. *Sivapithecus indicus*, GSP 30730; **i**. *Microcolobus* sp., KNM-NA 47916 A; **j**. *Caipora bambuiorum*, IGC-UFMG 05; **k**. *Ateles* sp., ZMB 45255; **l**. *Colobus guereza*, AMNH 52223; **m**. *Papio anubis*, USNM 384235; **n**. *Hylobates klossii*, AMNH 103344; **o**. *Pan troglodytes*, MPI-EVA 11778. The figured specimens are from the left side and are not to scale

Table 4 Linear measurements (in mm) of the left partial humerus of *Pliobates cataloniae* (IPS58443.15)

Variable	Measurement
Humerus length	>152.3
Distal epiphysis (proximodistal) length	33.3
Distal end to midshaft (proximodistal) length	65.0
Distal humerus articular (mediolateral) width	22.6
Distal humerus maximum (anteroposterior) depth	13.3
Trochlear maximum (mediolateral) width	8.0
Trochlear maximum (anteroposterior) depth	6.3
Capitulum maximum (mediolateral) width	6.0

of *Sivapithecus parvada*, which besides being overall larger and stouter is further retroflexed (with an anteriorly convex shaft and a marked medial shaft concavity; Pilbeam et al. 1990; Moyà-Solà and Köhler 1996; Köhler et al. 2001; Alba et al. 2011).

The flat and conical humeral trochlea of *Pliobates* (without spooling) shows similarities with that of *Aegyptopithecus*, dendropithecids, *Microcolobus* and *Epipliopithecus* (Fig. 3c–f), being markedly different from those of extinct crown (e.g., *Sivapithecus*) and extant hominoids (Fig. 3g–h, m–n), in which the trochlea is well developed and spool-shaped—a trait also observed, to a lesser extent, in the stem hominoid *Ekembo* (Fig. 3b)—with a deep trochlear groove, a markedly projecting medial keel (albeit less so in *Hylobates*), and a well-developed lateral keel (Bacon 2000; Alba et al. 2011; Takano et al. 2018). *Pliobates* has a well-developed zona conoidea, lacks a capitular tail, and displays a globular capitulum that does not expand posterolaterally, resembling the condition of crown and some stem hominoids (Fig. 3, g–h, m–n; Rose 1988; Alba et al. 2015). Likewise, *Pliobates* lacks an entepicondylar foramen, as in extant crown catarrhines (cercopithecoids and hominoids), the extinct atelid *Caipora*, extant atelids, stem hominoids, dendropithecids (Fig. 3a–e, g–n; Fleagle and Simons 1982; Rose 1997) and *Pliopithecus* (Alba and Moyà-Solà 2014), but unlike *Epipliopithecus* (Fig. 3f; Begun 2002) and *Aegyptopithecus* (Fleagle and Simons 1982; Gebo 1993). The radial fossa morphology of *Pliobates* generally resembles that of *Aegyptopithecus*, cercopithecoids (including *Microcolobus*), dendropithecids, and *Ekembo* (Fig. 3b–e, k–l; Fleagle and Simons 1982; Gebo 1993; Nakatsukasa et al. 2010; Alba et al. 2011; Takano et al. 2018) by being relatively deep and expanded, while being dissimilar to the reduced radial fossa and more developed (larger, rounder and deeper) coronoid fossa of extinct and extant crown hominoids (Fig. 3g–h, m–n; Rose 1997; Nakatsukasa and Kunimatsu 2009; Alba et al. 2011).

The long and deep medial epicondyle of *Pliobates* is similar to that of dendropithecids (Fig. 3c–e; Fleagle 1983) and somewhat like that of *Aegyptopithecus* in length and projection, particularly in posterior view, but differs from the latter and that of platyrrhines, which have a posteriorly retroflexed epicondyle that is more medially projecting (Fig. 3b, i–j; Fleagle and Simons 1982; Gebo 1993; Rosenberger et al. 2009; Tallman and Cooke 2016). The condition of *Pliobates* is also dissimilar from that of hominids, which have a large and medially projecting medial epicondyle; hylobatids, which display more projection than *Pliobates* but less so than hominids (Fig. 3h, m–n); and cercopithecoids (including the fossil colobine *Microcolobus*), which display a reduced and posteromedially oriented (to varying degrees) medial epicondyle (Fig. 3i, k–l; McHenry and Corruccini 1975; Senut 1986; Feldesman 1982; McCrossin et al. 1998; Bacon 2000; Nakatsukasa et al. 2010). The lateral epicondyle of *Pliobates* is similar to that of *Ateles* (small and only slightly laterally projecting; Fig. 3j) and differs from that of hominoids, in which the epicondyle is well developed and laterally protruding (Rosenberger and Strier 1989; Bacon 2000; Youlatos et al. 2015; Zelazny 2019). The olecranon fossa of *Pliobates* displays a similarly shallow condition to that of non-atelid platyrrhines, *Aegyptopithecus*, *Microcolobus*, *Epipliopithecus*, and dendropithecids (Fig. 3c–f; Fleagle and Simons 1982; Gebo 1993; Nakatsukasa et al. 2010; Tallman and Cooke 2016; Bouchet et al. 2024b), but differs from that of hominoids and atelids, which display deep fossae with sharp and well defined margins and with an articular surface that extends onto the fossa laterally (Rose 1997; Alba et al. 2011; Bouchet et al. 2024b).

Geometric morphometric analysis

The bgPCA based on the distal humerus discriminates among extant hominoids, cercopithecoids, and platyrrhines (Fig. 4). The analysis correctly classifies 100% of the extant specimens (98.6% after cross-validation) into the five previously defined groups (platyrrhines, colobines, cercopithecines, hylobatids, and hominids). The PERMANOVA results indicate that group differences are significant at $p<0.05$ for the landmark configurations, the bgPCA, and the cross-validated bgPCA. The Z-scores and R^2 values, as expected, are higher for the bgPCA ($Z=18.27$; $R^2=0.81$) than for the raw data ($Z=8.59$; $R^2=0.41$), but are very similar to the cross-validated bgPCA ($Z=17.72$; $R^2=0.80$)—overall indicating that grouping structure is not spurious. The first three bgPCs together account for 97% of the variance (Fig. 4), whereas the bgPC4 was not considered because it only accounts for 3% of the variance. Phylogenetic signal for the raw data when fossils are considered is significant but with $K<1$ values, contrary to when only extant taxa are considered ($K>1$; Table 5). The bgPC1 (62% of the variance) is not significantly correlated with ln CS ($p=0.104$) and embeds significant phylogenetic signal, being also $K>1$ when extant taxa are considered and $K<1$ when fossils are

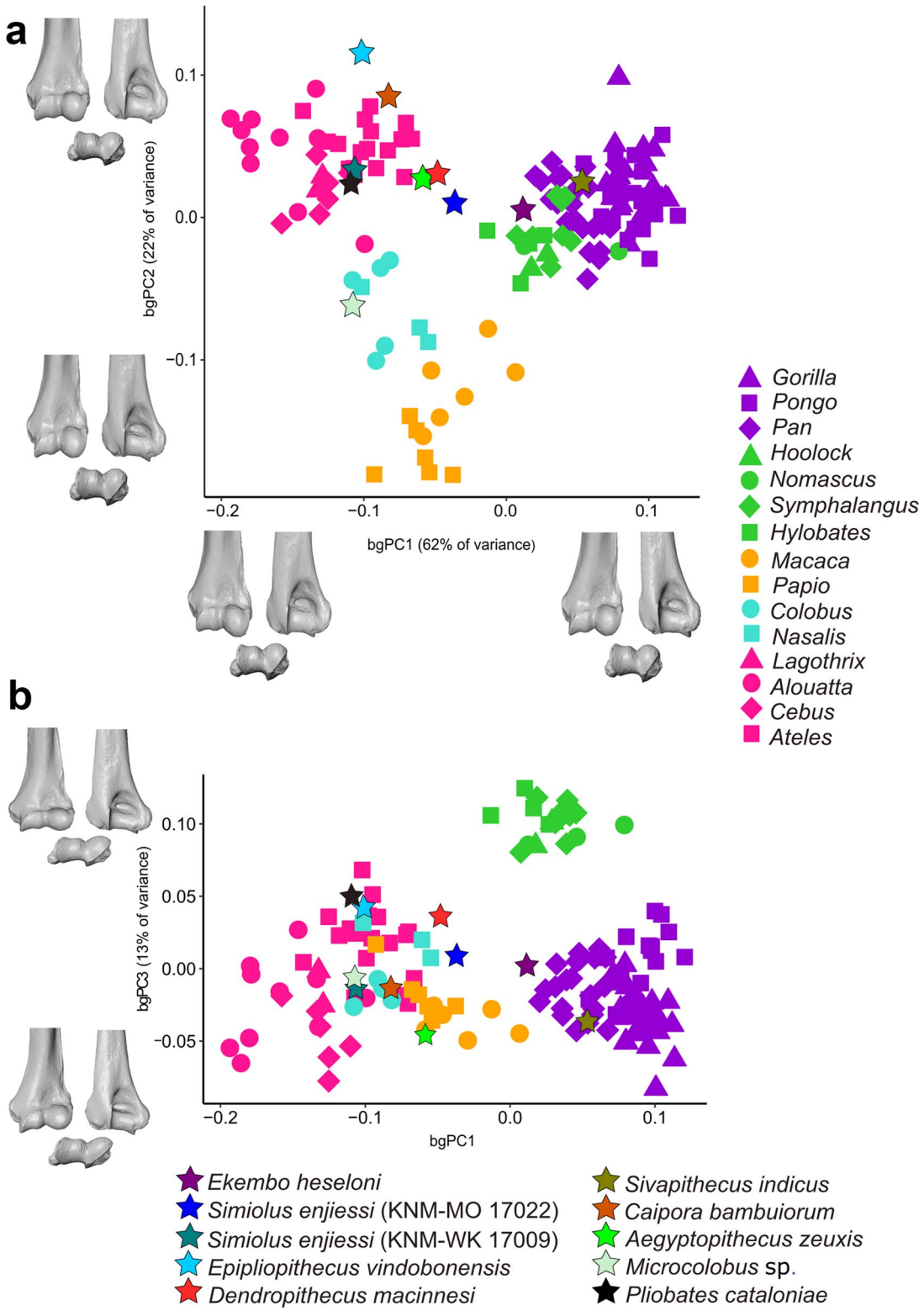

Fig. 4 Results of the bgPCA for the distal humerus, as represented by a bivariate plot of bgPC2 (**a**) and bgPC3 (**b**) vs. bgPC1. The percentage of variance is depicted within parentheses for each axis. The shape configurations at the end of each axis are depicted in anterior (top left), posterior (top right), and distal (bottom) views, and were warped onto the specimen closest to the mean, belonging to *Nasalis larvatus* (USNM 198276). A priori groups are color-coded: violet, hominids; green, hylobatids; orange, cercopithecines; turquoise, colobines; pink, platyrrhines. Fossil specimens (projected a posteriori) are denoted with colored stars

Table 5 Phylogenetic signal (as measured by Blomberg's *K*, with significance within parentheses) embedded by the first three bgPCs and the landmark configurations (after GPA) resulting from the bgPCA of distal humeral shape, based on the extant comparative sample only and further including the fossil specimens projected a posteriori

bgPC	Only extant taxa	Extinct and extant taxa
	K (p)	*K (p)*
bgPC1	2.92 (<0.001)	0.65 (<0.001)
bgPC2	1.65 (<0.001)	1.11 (<0.001)
bgPC3	1.85 (<0.001)	0.69 (<0.001)
Landmark configurations	1.37 (<0.001)	0.40 (<0.001)

included (Table 5). This axis clearly discriminates the a priori distinguished groups, with extant hominoids generally displaying positive scores and monkeys displaying negative scores with few exceptions (Fig. 4). There is, however, considerable overlap between hylobatids and hominids (particularly, *Symphalangus* and *Pan*), as well as between cercopithecines, colobines, and platyrrhines (particularly *Ateles*). The bgPC1 is driven by differences in the shape of the trochlea, the medial epicondyle and, to a lesser extent, the capitulum. Taxa with more positive scores (hominoids) exhibit a marked elevation of the medial keel of the trochlea, a well-defined lateral keel and a deeper zona conoidea, a medially projecting medial epicondyle, and a more rounded capitulum. In contrast, taxa with negative scores display a less pronounced or reduced elevation of the medial keel of the trochlea, a somewhat less defined lateral keel and a shallower zona conoidea, and a distally projecting and narrower capitulum. *Pliobates* shows a negative bgPC1 score, driven by the less projecting medial keel and medial epicondyle, thus overlapping with platyrrhines and the lower variation range of cercopithecoids. This condition also closely resembles *Simiolus* (KNM-WK 17009) and *Epipliopithecus*, and, to a lesser extent, *Caipora*, *Microcolobus*, *Dendropithecus*, *Aegyptopithecus*, and the other *Simiolus* specimen (KNM-MO 17022), which are relatively close to *Pliobates*. In contrast, the two extinct hominoids analyzed overlap with extant hominoids, with *Ekembo* displaying a mildly positive score most similar to that of hylobatids (due to the less marked projection of the medial keel), and *Sivapithecus* resembling both hylobatids and hominids (thus exhibiting a crown hominoid-like morphology of the trochlea, medial epicondyle, and capitulum).

Like the bgPC1, the bgPC2 (22% of the variance) is not correlated with ln CS ($p=0.312$) and embeds high ($K<1$) and significant phylogenetic signal with and without fossils (Table 5). This axis discriminates cercopithecoids (with the most negative scores) from both platyrrhines and hominoids (with moderately negative to positive scores), with only slight overlap between some colobines and the lower range of variation of hominoids (Fig. 4a). The bgPC2 is driven by the shape of the trochlea and the capitulum. Thus, in specimens with more positive scores the trochlea is somewhat spool-shaped (i.e., there is a slight trochlear groove and some projection of the medial keel—although not as much as in the positive extreme of bgPC1, corresponding to the morphology exhibited by hominoids alone) and the capitulum is globular and mediolaterally expanded. In contrast, in specimens with negative scores, the medial keel is projected, the trochlea is narrower mediolaterally and the zona conoidea is narrower; the capitulum is narrower and distally projecting. *Pliobates* displays moderately positive bgPC2 scores, similarly to the remaining fossil specimens (except for *Caipora* and *Epipliopithecus*, which show more extreme positive values, and *Microcolobus*, which displays more negative values, thus overlapping with the distribution of hominoids and platyrrhines). Most taxa fall around zero or positive values in bgPC2, while cercopithecoids, and papionins in particular, display the most negative scores—due to the markedly projecting medial keel of papionins (Fig. 3m), which is particularly pronounced in *Papio* (which has the most negative scores; Fig. 4a).

The bgPC3 (13% of the variance) is not correlated with ln CS either ($p=0.165$) and embeds significant phylogenetic signal both with and without fossils (Table 5), with high $K>1$ when the analysis is done without fossils and $K<1$ when fossils are included. The bgPC3 axis mainly discriminates hylobatids, which display the most positive scores, from great apes and monkeys, which all overlap and have a wide distribution between positive and negative scores. The bgPC3 is driven by differences in trochlear, medial epicondyle and capitulum shape. In particular, humeri with most positive scores (corresponding to hylobatids) exhibit a wider capitulum and a more marked projection of the lateral epicondyle than those at the negative end. In contrast, those displaying the most negative scores (platyrrhines, hominids, and cercopithecoids) show a shorter trochlea in the superior-inferior direction, an anterior projection of the medial keel, and a more rounded capitulum. Most of the fossils, including *Pliobates*, are placed around zero or in positive scores, although none of them approach hylobatids. *Pliobates* and *Epipliopithecus* fall in close proximity, overlapping mainly with *Ateles*, while one *Simiolus* (KNM-MO 17022), *Microcolobus* and *Ekembo* display scores around zero. The other *Simiolus* (KNM-WK 17009) and *Caipora* have slightly negative scores, although still close to zero, whereas the humeri of *Aegyptopithecus* and *Sivapithecus* display the most negative scores.

When bgPC2 and bgPC1 are considered simultaneously (Fig. 4a), *Pliobates* most closely resembles the *Simiolus* from Kalodirr, falling well within the area of the morphospace occupied by extant platyrrhines, overlapping with *Ateles* but not far from specimens of the remaining platyrrhine genera analyzed. When bgPC3 is further considered

(Fig. 4b), *Pliobates* mainly overlaps with platyrrhines as well as cercopithecoids (closer to colobines than to papionins), alongside other fossils to the exception of *Ekembo*, and *Sivapithecus* (which lay close by or overlap with hominids but not hylobatids). The overall closer similarities of the distal humerus of *Pliobates* with that of platyrrhines is confirmed by typicality probabilities (Table 6), which further show *Aegyptopithecus*, *Epipliopithecus*, dendropithecids and *Caipora* as having closest morphological affinities with platyrrhines—albeit one of the *Simiolus* specimens, together with *Aegyptopithecus* and *Epipliopithecus* fall outside the extant platyrrhine variation at $p<0.05$ (and thus are outliers for that group). *Microcolobus* shows affinities with both cercopithecines and colobines, but falls outside of the variation of both ($p<0.05$). In any case, *Pliobates* clearly differs from the extinct hominoids analyzed (including the stem hominoid *Ekembo*), which show affinities with hominids and fall within their extant range of variation.

Locomotor repertoire inference

The covariation between humeral shape and locomotor behavior is significant and strong (r-PLS = 0.82; $p<0.001$). The first axis (PLS1) explains 83.97% of the covariance between the blocks (Fig. 5a), while the second axis (PLS2) explains 10.05%; both are significant ($p<0.001$). The subsequent three axes each explain less than 5% of the covariance between blocks and, thus, are not considered further. The PLS1 distinguishes between clambering and leaping behaviors (positive end) and quadrupedalism (negative end; Fig. 5b). At the positive end, hylobatids display the most positive scores on the shape axis, whereas the two *Papio* (and cercopithecoids more broadly) occupy the negative extreme. The PLS2 distinguishes between quadrupedalism and climbing (positive end) and leaping and suspension (negative end). Great apes and papionins (except *Macaca mulatta*) fall at the negative end, whereas some platyrrhines and colobines (and *M. mulatta*) occupy the positive extreme, with most hylobatids and atelids displaying values around zero or moderately positive or negative ones (Online Resource 1: Fig. S2). Due to the relatively low covariance percentage and the equivocal taxa distribution and associated locomotor loadings (e.g., leaping/suspension in *Papio* and *Macaca* species), PLS2 was not used to estimate LMPs for the fossils and was not considered further. The MAE after LOOCV is 11.7%, indicating that our predictions are reasonably accurate (see Online Resource 1: Table S3 for details on the predictions of the extant and fossil taxa). Cross-validated errors computed per locomotor type indicate higher MAE for quadrupedalism (16.8%) and climbing (15.1%) and lower errors for leaping (7.6%) and suspensory (7.5%) behaviors. The MAE computed per species and across locomotor types (Online Resource 1: Table S4) indicate that great apes accumulate error in the QWR and CL categories, with QWR overall contributing the most with extreme MAE values for some taxa (African great apes, *Pongo* and hylobatids, and some cercopithecoids to a lesser extent). The CL and L locomotor types errors are high across different species, ranging from *Gorilla beringei* (44%) to *Macaca arctoides* (7%) or *Lagothrix lugens* (26%). The L and S categories per taxa are moderately high in some cases, such as *Colobus guereza* for L (with the highest error at 20%) and *Hylobates agilis* for S (with 32%). The species with lower error across categories are *Hylobates klossi*, with very low error across all locomotor types, *Alouatta palliatta*, *Cebus capucinus* and *Papio anubis*, and the analysis performs better for species with more generalized or stereotypical locomotor repertoires, such as non-atelid platyrrhines and cercopithecoids.

The estimated LMPs for the fossil sample are reported in Fig. 6 and in Online Resource 1: Table S3. The estimated locomotor repertoire for *Pliobates* includes a high proportion of suspensory behaviors (S = 37%), vertical climbing/clambering (CL = 24%), and leaping (L = 33%), with a comparatively minor quadrupedal component (QWR = 6%). The fossils with an estimated higher component of quadrupedalism (71–45%) are (in descending order) *Microcolobus*, *Aegyptopithecus*, *Ekembo*, *Sivapithecus*, *Simiolus*, and *Caipora*. *Dendropithecus* and *Epipliopithecus* are inferred to engage in moderately high amounts of climbing (> 30%).

Table 6 Typicality probabilities of group membership based on the bgPCA. Highest non-significant typicality probability for each taxon is in bold

Species (Catalog No.)	Cercopithecines	Colobines	Hominids	Hylobatids	Platyrrhines
Pliobates cataloniae (IPS58443)	< 0.001	0.001	< 0.001	< 0.001	**0.192**
Aegyptopithecus zeuxis (DPC-8702)	< 0.000	< 0.000	< 0.000	< 0.000	**0.016**
Cairpora bambuiorum (IGC-UFM605)	< 0.001	< 0.001	< 0.001	< 0.001	**0.060**
Dendropithecus macinnesi (KNM-RU 2097)	< 0.001	< 0.001	< 0.001	0.006	**0.059**
Ekembo heseloni (KNM-RU 2036AK)	< 0.001	< 0.001	**0.156**	0.006	< 0.001
Epipliopithecus vindoboniensis (NHMW 1970/1397/0003)	< 0.001	< 0.001	< 0.001	< 0.001	**0.017**
Microcolobus sp. (KNM-NA 47916 A)	**0.002**	0.001	< 0.000	< 0.000	< 0.000
Simiolus enjiessi (KNM-MO 17022 A)	< 0.001	0.001	0.001	0.004	**0.022**
Simiolus enjiessi (KNM-WK-17009)	< 0.001	< 0.001	< 0.001	< 0.001	**0.743**
Sivapithecus indicus (GSP 30730)	< 0.001	< 0.001	**0.847**	< 0.001	< 0.001

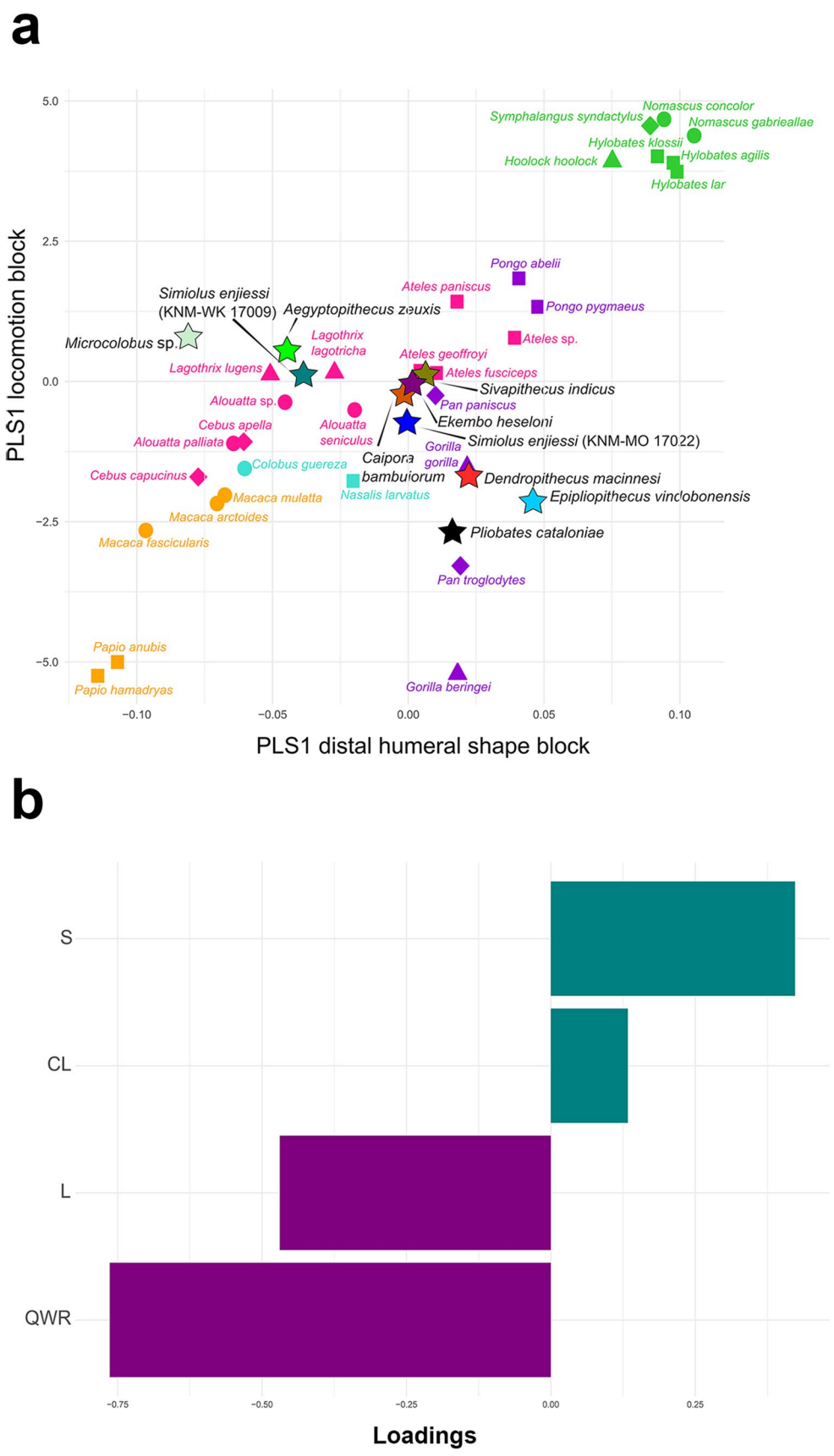

Fig. 5 **a**. Results of the two-block partial least squares analysis as depicted by a bivariate plot between the first axis (PLS1) of the locomotion block vs. that of distal humerus shape; **b**. loadings for the locomotor variables (LMPs) on PLS1. Fossil specimens were projected a posteriori and are indicated by stars. A priori groups are color-coded: violet, hominids; green, hylobatids; orange, cercopithecids; turquoise, colobines; pink, platyrrhines

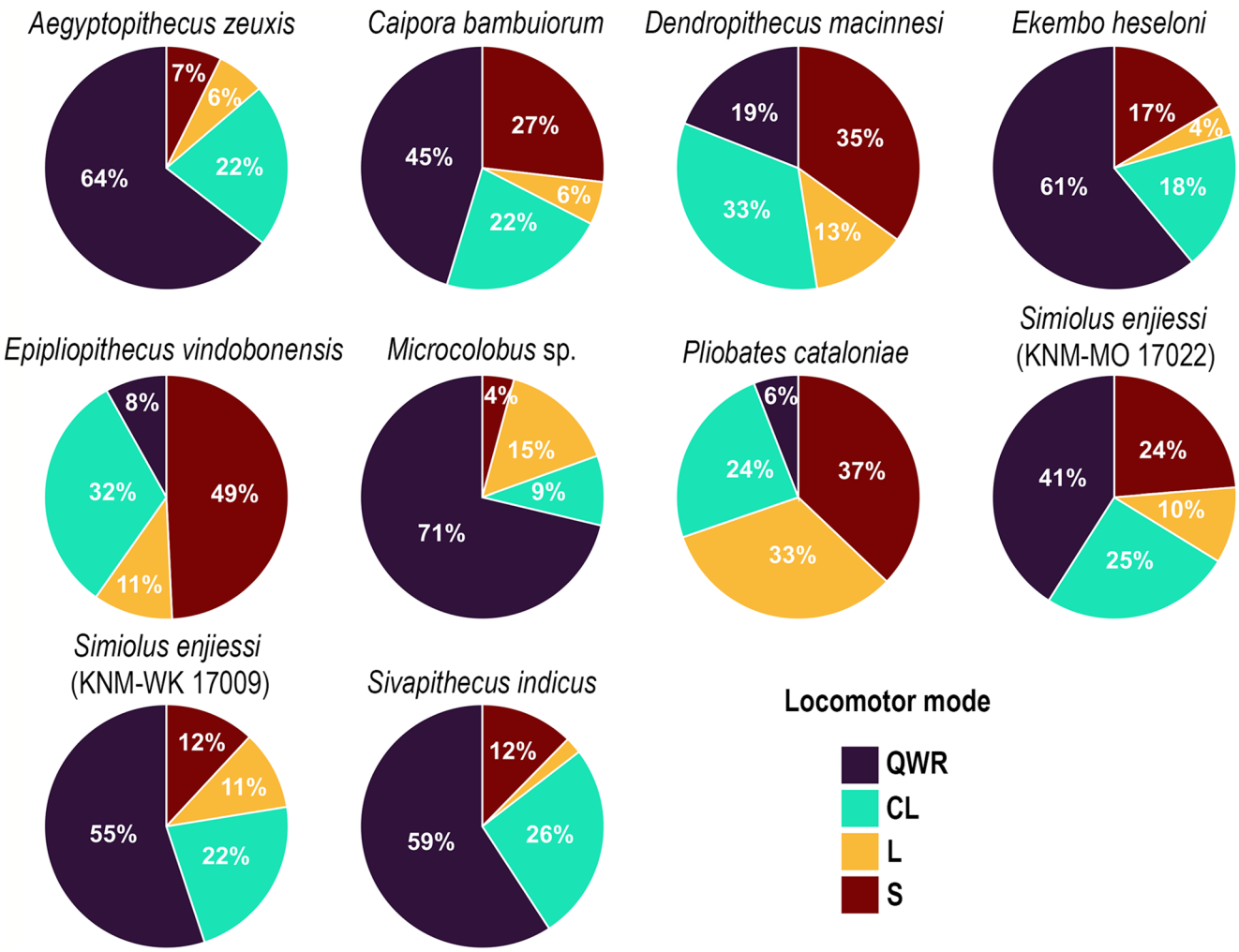

Fig. 6 Pie charts summarizing the estimated locomotor repertoires for the analyzed extinct taxa. See main text for abbreviations

The locomotor repertoire of *Epipliopithecus* (49%) includes a high proportion of suspensory behaviors, similar, albeit to a lesser extent, to *Dendropithecus* (35%)—which displays values similar to *Pliobates*.

Discussion

Morphofunctional and phylogenetic considerations

Our results indicate that the shape of the distal humerus embeds significant phylogenetic signal among extant anthropoids. The high Blomberg's *K* values obtained for the first two bgPCs when including only extant taxa indicate that the humeral distal shape tends to be conserved within the different extant clades, as evidenced by the marked separation between them (platyrrhines, hominoids, colobines, and cercopithecids). In this regard, the distal humerus of hominoids is characterized by a mediolaterally wider epiphysis, a rounded capitulum, and a large and spool-shaped trochlea, with a medially projecting medial epicondyle, as well as a deep zona conoidea; platyrrhines show a slightly pronounced medial trochlear keel, with a medial epicondyle that is also less projecting than in hominoids, and a narrower and more distally projecting capitulum; and, cercopithecoids have a mediolaterally narrow articulation, with a narrow and oval capitulum and a short trochlea, with a marked development of the medial keel. However, when fossils are included, *K* values drop significantly below 1 for bgPC1 and bgPC3, although they remain around 1 for bgPC2, revealing underlying homoplasy in the evolution of humeral traits in catarrhines. When the phylogenetic signal is explored using the whole shape (landmark configurations) of the distal humerus, Blomberg's *K* is also much lower, reinforcing the notion of a degree of homoplasy at play. Even in the case of bgPC2, and as remarked by Raventós-Izard et al. (2025), significant phylogenetic signal with high values of Blomberg's *K* would not be incompatible with making functional

inferences because locomotion may also be correlated with phylogeny; as such, we offer morphofunctional considerations regarding the distal humerus of *Pliobates cataloniae* below.

Our comparisons indicate that the humeral shaft and humeroulnar articulation of *Pliobates* most closely resembles, among extant anthropoids, the condition of platyrrhine monkeys. The humeral shaft, in particular, is anteriorly straight and somewhat retroflexed proximally, resembling the morphology of *Cebus* and the pliopithecoid *Epipliopithecus* (Zapfe 1958, 1961; Rose 1994, 1997; Arias-Martorell et al. 2015). Contrarily, *Ekembo* (and Miocene apes from Africa more broadly, including, e.g., *Afropithecus*, *Equatorius* and *Nacholapithecus*, albeit all taxa display shaft morphology differences among each other; Alba et al. 2011) displays more humeral shaft retroflexion compared with *Pliobates*, with a slight flattening at its distal portion and a triangular cross section on its proximal portion as a result of a well-defined deltoid plane (Alba et al. 2011). At the humeroulnar articulation, the distal humeral shape of *Pliobates* is characterized by a slightly pronounced medial keel, a poorly defined lateral trochlear keel, and the absence of spooling at the trochlea, thus resembling extant platyrrhines and lacking the mechanisms for passive stabilization during flexion and extension that are characteristic of extant hominoids (Szalay and Dagosto 1980; Rose 1988). *Aegyptopithecus*, *Epipliopithecus*, *Dendropithecus*, and *Caipora* are similar to *Pliobates* in this regard, also exhibiting the characteristics found in extant platyrrhine monkeys (Fleagle 1983; McCrossin and Benefit 1997; Perry et al. 2018), whereas *Microcolobus* is unlike *Pliobates* and the other stem catarrhines by exhibiting a more colobine-like morphology of the distal humerus—with, e.g., a moderately globular capitulum and a somewhat reduced medial keel (a trait shared with extant colobines; Fig. 3i, l; Nakatsukasa et al. 2010). Feldesman (1982) already suggested that the distal humeri of Miocene stem catarrhines might resemble quadrupedal platyrrhines with suspensory capabilities more than extant catarrhines. On the other hand, *Ekembo* and *Sivapithecus* show more derived distal humeri, similar to those of extant hominoids. *Ekembo* is characterized by a relatively prominent medial trochlear keel (although not to the degree of extant hominoids) and pronounced lateral keel (Harrison 1987; Walker 1997). The configuration of the humeroulnar articulation of *Pliobates*, as inferred from distal humeral shape, is thus in agreement with its proximal ulnar shape (Raventós-Izard et al. 2025), which resembles that of *Ateles* and stem catarrhines such as *Aegyptopithecus*, *Dendropithecus*, *Simiolus*, and *Epipliopithecus* in its relatively narrow trochlear notch, which would have made it difficult to withstand transverse forces during pronation-supination. Therefore, the humeroulnar articulation of *Pliobates* differs from that of hominoids (including stem hominoids), where the wide and keeled trochlear notch (i.e., median keel) of the ulna and the corresponding trochlear spooling (i.e., flaring medial and lateral keels and deep trochlear groove) of the humerus provide joint stability during flexion-extension and pronation-supination movements (Rose 1988, 1997; Begun 1992; Alba et al. 2011).

For the radiohumeral articulation, *Pliobates* shows a moderately globular capitulum and a well-defined zona conoidea, resembling more the derived (ape-like) condition exhibited by hominoids, contrary to the more plesiomorphic humeroulnar joint. In this regard, *Microcolobus* possesses a relatively well-defined zona conoidea and, as indicated above, a moderately globular capitulum, similar to the stem hominoid *Ekembo*. These traits are even more markedly derived in *Sivapithecus*. The other stem catarrhines and *Caipora* display varying degrees of globularity in the capitulum (from very slight in *Caipora* and *Simiolus*, to more prominent in *Dendropithecus* and *Epipliopithecus*), but all have a smooth transition between the trochlea and the capitulum—i.e., a poorly defined zona conoidea. The condition of *Pliobates*, *Microcolobus* and hominoids (and stem hominoids to a lesser extent) is functionally linked to providing stability to the radial head during pronation and supination movements (Harrison 1987; Rose 1988; Walker 1997; Nakatsukasa et al. 2010; Pallas et al. 2026). Evidence from the radius does suggest that *Pliobates* would have engaged in highly efficient prono-supination, as indicated by its round and beveled radial head (Alba et al. 2015; Arias-Martorell et al. 2026). On the other hand, dendropithecids and *Epipliopithecus* exhibit a more oval radial head with a lateral lip (to varying degrees), more closely resembling the stem catarrhine ancestral condition (Arias-Martorell et al. 2021, 2023, 2026), in agreement with the more generalized shape of their humeral capitulum. The stem hominoids *Ekembo* and *Nacholapithecus* (for a discussion of its phylogenetic uncertainties, see Urciuoli and Alba 2023) show intermediate proximal radial morphologies (Arias-Martorell et al. 2023), indicating that their elbow might have been more stable during pronated (weight-bearing) positions while exhibiting enhanced prono-supination abilities.

Locomotor inferences

The low MAE of the PLSR indicates that the predictions of the model are reasonable accurate. However, when predictions for extant taxa are compared with the percentages compiled from the literature, there are some instances of overestimating quadrupedalism (QWR)—e.g., in the atelid *Lagothrix* and the hominid *Pongo*, the latter being mainly suspensory (Online Resource 1: Tables S2 and S3). In some taxa, quadrupedalism is also underestimated, such as in *G.*

beringei and *Pan troglodytes*. The contrary applies to suspension, where the predicted values are much lower for *Pongo* and most hylobatids (except *Hylobates lar*) than those compiled from the literature (Online Resource 1: Tables S2 and S3). The higher MAE errors for QWR and CL (~15–17%) and lower errors for L and S behaviors (~7–8%) suggest that the model more reliably captures locomotor modes that may be associated with more distinctive morphological correlates, whereas more generalized behaviors are predicted with greater uncertainty. In particular, QWR and CL likely encompass a range of sublocomotor styles due to, e.g., variations in substrate use, limb loading, positional behavior, etc., introducing greater heterogeneity within these categories and reducing predictive accuracy. African great apes accumulate the most error for QWR (Online resource Table S3 and S4); they rely on knuckle-walking while on the ground, which allows African great apes to retain morphological features for suspensory locomotion (e.g., finger length; Inouye 1994; Kivell and Smith, 2009; Schmitt et al. 2016)—therefore, the morphology exhibited by these taxa does not correspond to the expected morphology of a quadruped, which may destabilize the model. A comprehensive phylogenetic coverage of locomotor diversity across primates is the ideal approach to maximize representativeness and ameliorate some of the exposed shortcomings of the approach. However, the nature of the locomotor data used (which are potentially biased, e.g., if the full locomotor repertoire of a taxon is unknown, only some aspects such as arboreal behaviors have been studied or the limited number of species for which detailed locomotor data is available) and the sample included in the study (from which the predictions are derived) also affect the accuracy and reliability of the results.This is not an intrinsic limitation of the PLSR approach itself, but rather a general constraint of any predictive modelling framework. In any case, the locomotor frequencies predicted for the fossils should not be interpreted at face value but are merely indicative of general patterns. These considerations do not preclude making inferences for the fossils, provided that the results are critically contrasted with functional considerations. Likewise, such inferences should be also compared with those derived from other anatomical areas, which might contribute essential information on locomotor behaviors for which the distal humerus does not have sufficient predictive power.

The results for the locomotor frequency analysis of the distal humerus indicate that the locomotor repertoire of *Pliobates* would have included an important proportion of suspension, climbing/clambering, and leaping, while displaying a very small proportion of quadrupedalism (Fig. 7). These results are in moderate agreement with previous estimates (Raventós-Izard et al. 2025) regarding the amount of suspension, while diverging in the higher leaping and lower quadrupedalism frequencies inferred. In particular, based on distal humeral shape we infer 33% of leaping behaviors, while they were quite low (1–15%) based on both proximal and distal ulnar and radial shape (Raventós-Izard et al. 2025; Arias-Martorell et al. 2026). Quadrupedalism, on the other hand, is estimated in low percentages (7%), while they were high for the proximal ulna (47%) and distal radius (35%), but not for the distal ulna (0%) or the proximal radius (2%; Raventós-Izard et al. 2025; Arias-Martorell et al. 2026). The estimated percentages of suspension (35%) and climbing (21%), in turn, are not very different from those inferred from the ulna (29% and 38%, respectively), but differ widely from those inferred for the proximal (50%) and distal (14%) radius (Arias-Martorell et al. 2026).

Our findings support previous inferences for the fossils *Caipora*, *Dendropithecus*, and *Epipliopithecus*, which have been likened to suspensory atelids—*Caipora* to *Ateles* (Halenar 2011), and *Dendropithecus* and *Epipliopithecus* to *Lagothrix* (Arias-Martorell et al. 2015, 2021; Rein et al. 2015). The propliopithecoid *Aegyptopithecus* displays some affinities to the platyrrhines but it is an outlier for the shape variation of the group; its inferred locomotor repertoire—with high frequency of quadrupedalism (64%) combined with climbing (22%)—agrees well with previous inferences, which characterized *Aegyptopithecus* as a slow-moving arboreal quadruped and climber (Fleagle and Simons, 1982; Simons, 1995). The locomotor repertoire of *Microcolobus* has been inferred as including flexed-elbow quadrupedalism (for running and bounding) and lacking specialized suspensory adaptations (Nakatsukasa et al. 2010; Pallas et al. 2026), which agrees with the locomotor frequencies found in this study (71% quadrupedalism and 4% suspension). Regarding the stem hominoid *Ekembo*, the locomotor repertoire here inferred for this taxon (53% of quadrupedalism) also generally agrees with previous inferences, indicative of arboreal, powerful-grasping pronograde quadrupedalism without suspension (Kelley 1997; Rose 1997; Ward 1993, 1998, 2015; Daver and Nakatsukasa 2015). The locomotor inferences for *Si. indicus*, indicative of quadrupedalism combined with climbing and clambering, are also broadly in agreement with previous inferences (Pilbeam et al. 1990; Moyà-Solà and Köhler 1996; Richmond and Whalen 2001). Its humerus is more gracile overall than that of the larger *Si. parvada*, and more similar to that of *Hispanopithecus* and orangutans, thus probably being more adapted for arboreal behaviors such as climbing (Moyà-Solà and Köhler 1996). In contrast, *Si. parvada* might have engaged in more terrestrial quadrupedalism according to the morphology of the humeral shaft (with more marked humeral shaft retroflexion and medial convexity, like in terrestrial quadrupedal primates; Pilbeam et al. 1990; Richmond and Whalen 2001).

Fig. 7 Reconstruction of the locomotor repertoire exhibited by *Pliobates cataloniae*, based on previous papers and our results for the humerus presented in this paper. The presence of a tail in *Pliobates* (as well as its length and aspect) is currently unknown, although its stem catarrhine status suggests it would have had one. Artwork by JG

However, our results suggest that *Si. indicus* would have also engaged in quadrupedalism to some extent.

Regarding suspension in *Pliobates*, the length of the humerus (relative to the breadth of the distal end) and its gracile shape, combined with a relatively long radius and the carrying angle of the elbow (9.8 degrees; Alba et al. 2015) are consistent with the use of suspensory behaviors in this taxon. However, due to the more plesiomorphic condition of its humeroulnar joint compared with extant hominoids, a reliance on forelimb-dominated suspensory behaviors may be discounted for this taxon. This is most evident regarding hylobatid-like brachiation—i.e., a locomotor mode using bimanual strides where the full body weight is borne by the forelimbs without hindlimb or tail aid (Cant et al. 2001). This is because the *Pliobates* elbow lacks passive stabilization mechanisms such as the medial keel of the humeral trochlea (and its counterpart, the median keel of the ulna; Raventós-Izard et al. 2025). In contrast, *Pliobates* exhibits a derived (ape-like) condition of the humeroradial joint (Arias-Martorell et al. 2026), which is functionally related to enhanced prono-supination capabilities of the forearm (Rose 1983, 1988, 1993a, 1993b, 1997; Arias-Martorell et al. 2023). The ape-like humeral capitulum of *Pliobates*, instead of representing an adaptation to forelimb-dominated suspension, might be the result of selection pressures related to other arboreal behaviors that also required enhanced prono-supination, such as climbing and clambering (Fig. 7; Arias-Martorell et al. 2026: fig. 7). In hominoids, greater reliance on forelimb prono-supination has been linked to loss of external tail (Kelley 1997; Ward et al. 1991; Drapeau 2008; Nakatsukasa et al. 2003, 2004). No caudal vertebral remains have been found for any pliopithecoid to date, and Zapfe (1958, 1961) concluded that *Epipliopithecus* lacks and external tail based on the morphology of the sacrum. Subsequent authors (Ankel 1965; Russo 2016), however, disputed such conclusions, in agreement with its stem catarrhine status. There are no caudal or sacral remains of *Pliobates* to date, but as a stem catarrhine, it is best hypothesized as possessing an external tail. Thus, we have reconstructed the tail of *Pliobates* as being moderate in length given our

results and previous inferences about its locomotor repertoire (Fig. 7).

The high leaping frequency estimated for *Pliobates* based on the distal humeral shape is surprising, because it is not found for any of the other extinct taxa analyzed (next highest leaping taxon is *Microcolobus*, at 15%) or estimated based on the proximal ulna (Raventós-Izard et al. 2025) or radius (Arias-Martorell et al., 2026). Gibbons exhibit non-negligible frequencies of leaping (>15%) combined with ricochetal brachiation and climbing/clambering behaviors, alongside a virtual absence of quadrupedal locomotion (Fleagle 1976; Channon et al. 2010). The suspensory atelids similarly engage in moderate amounts of leaping behaviors (Mittermeier and Fleagle 1976; Mittermeier 1978; Cant et al. 2001) alongside some cercopithecoids (e.g., *Nasalis*; Napier and Napier 1967; Byron and Covert 2004; Su and Jablonski 2009). The fossil *Microcolobus* has also been inferred to engage in (non-specialized) leaping behaviors based on its femoral morphology (Nakatsukasa et al. 2010). However, the locomotor repertoire estimated for *Pliobates* based on the distal humerus does not fit well with any of these extant or fossil primates, differing from hylobatids in the higher reliance on leaping and orthograde behaviors other than suspension, from atelids in the higher reliance on leaping and suspensory behaviors (at the expense of quadrupedalism), and from leaping cercopithecoids (including *Microcolobus*) in the higher amounts of climbing and clambering. There is some evidence of forelimb and, particularly, humeral shaft features functionally related to leaping in primates generally, such as humeral diaphyseal strength (e.g., Ruff 2002; Ruff et al. 2019). However, primate leaping adaptations are mostly found in the hindlimbs (Walker 1974; Jouffroy and Lessetieur 1979; Jungers 1979; Preuschoft 1990; Ruff and Runestad 1992; Godfrey et al. 1995; Rafferty and Ruff 1994; Channon et al. 2010; Monclús-Gonzalo et al. 2025b). In this regard, the analysis appears to interpret as leaping correlates some elbow features that are functionally related to other behaviors, such as climbing, even if compatible with leaping. This is the case of the ape-like humeroradial joint (and associated musculature anatomy and recruitment pattern), which result in efficient prono-supination—useful for rotating the forearm during climbing, suspension, and leaping alike (Szalay and D'Agosto 1980; Rose 1983, 1988; Stern and Larson 2001; Vanhoof et al. 2020, 2021). This is supported by the fact that the leaping percentages of hylobatids and, especially, *Nasalis* and atelids are overestimated by our analyses (Online Resource 1: Tables S2 and S3). Therefore, a detailed analysis of the hindlimb remains of *Pliobates* would be needed to more conclusively ascertain the leaping frequencies displayed by this taxon.

Conclusions

The left distal humerus of *Pliobates* is morphologically more similar to the distal humeri of platyrrhines and stem catarrhines but further displays some features (such as a globular capitulum) that indicate a higher mobility of the elbow joint. The locomotor repertoire of *Pliobates* inferred from the distal humerus does not have any clear extant analog and does not compare directly to any other fossil catarrhines included in the analyses. Based on the combined evidence from the whole elbow joint, *Pliobates* might have mostly relied on arboreal climbing and clambering, further combining these behaviors with quadrupedalism, non-acrobatic suspension, and, maybe, some degree of leaping (Fig. 7). The distal humeral features associated with leaping are also functionally related to climbing, clambering, and suspension, so that further studies of the hindlimb remains would be required to confirm that leaping was a non-negligible component of the *Pliobates* locomotor repertoire. Finally, some degree of forelimb-dominated suspension cannot be entirely discounted for *Pliobates*. However, the great range of prono-supination at the humeroradial joint might alternatively be related to other locomotor behaviors that also benefit from efficient prono-supination, such as climbing and clambering. In any case, given the lack of ape-like stabilizing mechanisms at the elbow joint in *Pliobates*, such forelimb-dominated behaviors (if present) would have differed from the acrobatic suspension displayed by atelids and hylobatids.

Supplementary Information The online version contains supplementary material available at https://doi.org/10.1007/s10914-026-09828-0.

Acknowledgements The µCT scans of *Pliobates* were performed at the CENIEH with the collaboration of the CENIEH staff. We thank S. Siarabi for her assistance taking pictures of the remains of *Pliobates*. We would like to thank M. Nakatsukasa and L. Pallas for sharing the 3D model of KNM-NA 47916 A. We would also like to thank three anonymous reviewers and the Guest Editor (M. Pina) for their comments, which helped improve earlier versions of the manuscript. We dedicate this work to S. Moyà-Solà, in recognition of all his contributions to paleoprimatology (particularly, in the study of *Pliobates*) and for taking Catalan Paleontology to new heights of excellence and visibility—none of this would exist without you, Salva.

Author contributions J.A.M. and A.F.T. contributed equally to this work. J.A.M. and A.F.T. designed the study. J.A.M., A.F.T., T.A.P. and S.A. gathered the data. J.A.M., A.F.T., T.A.P., G.R.I. and A.U. selected the methods and performed the analyses. J.A.M., A.F.T., T.A.P. and D.M.A. interpreted the results. J.A.M., A.F.T. and T.A.P. prepared the figures. J.G. provided the illustrations included in this work. J.A.M., A.F.T. and D.M.A. wrote the manuscript with input from all other authors.

Funding Open Access funding provided by CERCA through the CRUE-CSIC agreement with Springer Nature. This publication is part of the R+D+I projects PID2020-116908GB-100, PID2020-117289GB-100, and PID2024-159434NB-I00, funded by Ministerio de Ciencia, Innovación y Universidades/Agencia Estatal de Investigación/10.13039/501100011033 and FEDER, EU. Research has also been funded by the Generalitat de Catalunya/CERCA Programme; the Agència de Gestió d'Ajuts Universitaris i de Recerca of the Generalitat de Catalunya (Consolidated research groups 2022 SGR 00620 and 2022 SGR 01188); the Departament de Cultura of the Generalitat de Catalunya (ARQ001SOLC-241-2025); a predoctoral grant from the Ministerio de Ciencia e Investigación (PRE2021-09911) to G.R.I.; and a predoctoral grant (CT22/25) from the Complutense University of Madrid to A.F.T.

Data availability The fossil material of *Pliobates* analyzed in this paper is housed and adequately curated in ICP, and it is available for study to other researchers. All the relevant data used for and generated from this study are included in the paper or in Online Resource 1. 3D models of extant comparative taxa can be found in MorphoSource (www.morphosource.org) and accessed by their catalog number listed in Online Resource: Table S1 and through the following link: https://www.morphosource.org/projects/00000C706/ (Primate Phenotypes project; Almécija et al. 2024). A 3D model of the distal humerus of *Pliobates* can also be found in MorphoSource (https://doi.org/10.17602/M2/M768930). The 3D models of extant taxa not deposited to MorphoSource are available upon request.

Declarations

Competing interests The authors declare no competing interests.

Conflict of interest The authors declare no conflict of interest.

References

Adams DC (2014) A method for assessing phylogenetic least squares models for shape and other high-dimensional multivariate data. Evolution 68:2675–2688. https://doi.org/10.1111/evo.12463

Adams DC, Collyer ML, Kaliontzopoulou A, Baker E (2022) geomorph: Geometric Morphometric Analyses of 2D/3D Landmark Data. R package version 4.0.4. https://cran.r-project.org/web/packages/geomorph/index.html

Alba DM (2012) Fossil apes from the Vallès-Penedès Basin. Evol Anthropol 21:254–269. https://doi.org/10.1002/evan.21312

Alba DM, Moyà-Solà S (2014) New fossil remains of *Pliopithecus canmatensis* from Abocador de Can Mata, and their implications for the taxonomic validity and phylogenetic position of *Epipliopithecus* (Primates, Pliopithecidae). Am J Phys Anthropol 153:64

Alba DM, Moyà-Solà S, Almécija S (2011) A partial hominoid humerus from the Middle Miocene of Castell de Barberà (Vallès-Penedès Basin, Catalonia, Spain). Am J Phys Anthropol 114:365–381. https://doi.org/10.1002/ajpa.21417

Alba DM, Almécija S, DeMiguel D, Fortuny J, Pérez de los Ríos M, Pina M, Robles JM, Moyà-Solà S (2015) Miocene small-bodied ape from Eurasia sheds light on hominoid evolution. Science 350:aab2625. https://doi.org/10.1126/science.aab2625

Alba DM, Casanovas-Vilar I, Garcés M, Robles JM (2017) Ten years in the dump: An updated review of the Miocene primate-bearing localities from Abocador de Can Mata (NE Iberian Peninsula). J Hum Evol 102:12–20. https://doi.org/10.1016/j.jhevol.2016.09.012

Alba DM, Robles JM, Casanovas-Vilar I, Beamud E, Bernor RL, Cirilli O, DeMiguel D, Galindo J, Llopart I, Pons-Monjo G, Sánchez IM, Vinuesa V, Garcés M (2022) A revised (earliest Vallesian) age for the hominoid-bearing locality of Can Mata 1 based on new magnetostratigraphic and biostratigraphic data from Abocador de Can Mata (Vallès-Penedès Basin, NE Iberian Peninsula). J Hum Evol 170:103237. https://doi.org/10.1016/j.jhevol.2022.103237

Almécija S, Alba DM, Moyà-Solà S (2009) *Pierolapithecus* and the functional morphology of Miocene ape hand phalanges: paleobiological and evolutionary implications. J Hum Evol 57:284–297. https://doi.org/10.1016/j.jhevol.2009.02.008

Almécija S, Tallman M, Alba DM, Pina M, Moyà-Solà S, Jungers WL (2013) The femur of *Orrorin tugenensis* exhibits morphometric affinities with both Miocene apes and later hominins. Nat Commun 4:2888. https://doi.org/10.1038/ncomms3888

Almécija S, Orr CM, Tocheri MW, Patel BA, Jungers WL (2015) Exploring phylogenetic and functional signals in complex morphologies: The hamate of extant anthropoids as a test-case study. Anat Rec 298:212–229. https://doi.org/10.1002/ar.23079

Almécija S, Pugh KD, Anaya A, Smith CM, Simmons NB, Voss RS, Duncan N, Lunde DP, Viera MK, Hsu T, Gilissen E (2024) Primate Phenotypes: A multi-institution collection of 3D morphological data housed in MorphoSource. Sci Data 11:1391. https://doi.org/10.1038/s41597-024-04261-5

Andrews P, Simons EL (1977) A new African Miocene gibbon-like genus, *Dendropithecus* (Hominoidea, Primates) with distinctive postcranial adaptations: its significance to origin of Hylobatidae. Folia Primatol 28:161–169. https://doi.org/10.1159/000155807

Andrews P, Harrison T, Delson E, Bernor RL, Martin L (1996) Distribution and biochronology of European and Southwest Asian Miocene catarrhines. In: Bernor RL, Fahlbusch V, Mittmann HW (eds) The Evolution of Western Eurasian Neogene Mammal Faunas. Columbia University Press, New York, pp 168–207

Ankel F (1965) Der Canalis sacralis als Indikator für die Länge der Caudalregion der Primaten. Fol Primatol 3:263–276. https://doi.org/10.1159/000155038

Arias-Martorell J, Alba DM, Potau JM, Bello-Hellegouarch G, Pérez-Pérez A (2015) Morphological affinities of the proximal humerus of *Epipliopithecus vindobonensis* and *Pliopithecus antiquus*: suspensory inferences based on a 3D geometric morphometrics approach. J Hum Evol 80:83–95. https://doi.org/10.1016/j.jhevol.2014.08.012

Arias-Martorell J, Almécija S, Urciuoli A, Nakatsukasa M, Moyà-Solà S, Alba DM (2021) A proximal radius of *Barberapithecus huerzeleri* from Castell de Barberà: Implications for locomotor diversity among pliopithecoids. J Hum Evol 157:103032. https://doi.org/10.1016/j.jhevol.2021.103032

Arias-Martorell J, Urciuoli A, Almécija S, Alba DM, Nakatsukasa M (2023) The radial head of the Middle Miocene ape *Nacholapithecus kerioi*: Morphometric affinities, locomotor inferences, and implications for the evolution of the hominoid humeroradial

joint. J Hum Evol 178:103345. https://doi.org/10.1016/j.jhevol.2023.103345
Arias-Martorell J, Raventós-Izard G, Monclús-Gonzalo O, Urciuoli A, Gamarra J, Nakatsukasa, Moyà-Solà S, Alba DM (2026) Apelike locomotor adaptations in the radius of the stem catarrhine *Pliobates* shed light on hominoid evolution. iScience 29:114622. https://doi.org/10.1016/j.isci.2025.114622
Aristide L, Strauss A, Halenar-Price LB, Gilissen E, Cruz FW, Cartelle C, Rosenberger AL, Topes RT, dos Reis SF, Perez I (2019) Cranial and endocranial diversity in extant and fossil atelids (Platyrrhini: Atelidae): A geometric morphometric study. Am J Phys Anthropol 169:322–331. https://doi.org/10.1002/AJPA.23837
Arnold C, Matthews LJ, Nunn CL (2010) The 10kTrees website: A new online resource for primate phylogeny. Evol Anthropol 19:114–118. https://doi.org/10.1002/evan.20251
Bacon AM (1994) Nouvelles perspectives sur la locomotion de *Pliopithecus vindobonensis* (Zapfe et Hüerzeler, 1957). C R Acad Sci Paris 318:259–266
Bacon AM (2000) Principal components analysis of distal humeral shape in Pliocene to Recent African hominids: The contribution of geometric morphometrics. Am J Phys Anthropol 111:479–487. https://doi.org/10.1002/(SICI)1096-8644(200004)111:4%3C479::AID-AJPA4%3E3.0.CO;2-%23
Begun DR (1988) Catarrhine phalanges from the late Miocene (Vallesian) or Rudabánya, Hungary. J Hum Evol 17:413–438. https://doi.org/10.1016/0047-2484(88)90030-9
Begun DR (1992) Phyletic diversity and locomotion in primitive European hominids. Am J Phys Anthropol 87:311–340. https://doi.org/10.1002/ajpa.1330870307
Begun DR (1993) New catarrhine phalanges from Rudabánya (Northeastern Hungary) and the problem of parallelism and convergence in hominoid postcranial morphology. J Hum Evol 24:373–402. https://doi.org/10.1006/jhev.1993.1028
Begun DR (2002) The Pliopithecoidea. In: Hartwig WC (ed) The Primate Fossil Record. Cambridge University Press, Cambridge, pp 221–240
Begun DR (2009) Dryopithecins, Darwin, de Bonis, and the European origin of the African apes and human clade. Geodiversitas 31:789–816. https://doi.org/10.5252/g2009n4a789
Begun DR (2017) Evolution of the Pliopithecoidea. In: Fuentes A (ed) The International Encyclopedia of Primatology. John Wiley & Sons, Chichester. https://doi.org/10.1002/9781119179313.wbprim0165
Blomberg SP, Garland T, Ives AR (2003) Testing for phylogenetic signal in comparative data: behavioral traits are more labile. Evolution 57:717–745. https://doi.org/10.1111/j.0014-3820.2003.tb00285.x
Bookstein FL (1991) Morphometric Tools for Landmark Data: Geometry and Biology, 1st ed. Cambridge University Press, Cambridge
Bookstein FL (2019) Pathologies of between-groups principal components analysis in geometric morphometrics. Evol Biol 46:271–302. https://doi.org/10.1007/s11692-019-09484-8
Bouchet F, Urciuoli A, Beaudet A, Pina M, Moyà-Solà S, Alba DM (2021) Comparative anatomy of the carotid canal in the Miocene small-bodied catarrhine *Pliobates cataloniae*. J Hum Evol 161:103073. https://doi.org/10.1016/j.jhevol.2021.103073
Bouchet F, Zanolli C, Skinner MM, Urciuoli A, Fortuny J, Almécija S, Bernardini F, Tuniz C, Schillinger B, Moyà-Solà S, Alba DM (2024a) Molar enamel–dentine junction shape of *Pliobates cataloniae* and other Iberian pliopithecoids. J Hum Evol 195:103581. https://doi.org/10.1016/j.jhevol.2024.103581
Bouchet F, Zanolli C, Urciuoli A, Almécija S, Fortuny J, Robles JM, Beaudet A, Moyà-Solà S, Alba DM (2024b) The Miocene primate *Pliobates* is a pliopithecoid. Nat Commun 15:2822. https://doi.org/10.1038/s41467-024-47034-9
Bouchet F, Zanolli C, Fotuny J, Moyà-Solà S, Alba DM (2025) Further insigth into an unnamed, medium-sized crouzeliid pliopithecoid from the Vallès-Penedès Basin (NE Iberian Peninsula). Swiss J Palaeontol 144:58. https://doi.org/10.1186/s13358-025-00404-2
Byron CD, Covert HH (2004) Unexpected locomotor behaviour: brachiation by an Old World monkey (*Pygathrix nemaeus*) from Vietnam. J Zool 263:101–106.
Cant JGH, Youlatos D, Rose MD (2001) Locomotor behavior of *Lagothrix lagothricha* and *Ateles belzebuth* in Yasuní National Park, Ecuador: general patterns and nonsuspensory modes. J Hum Evol 41:141–166. https://doi.org/10.1006/jhev.2001.0485
Cardini A, Polly PD (2020) Cross-validated between group PCA scatterplots: A solution to spurious group separation? Evol Biol 47:85–95. https://doi.org/10.1007/s11692-020-09494-x
Cartelle C, Hartwig WC (1996) A new extinct primate among the Pleistocene megafauna of Bahia, Brazil. Proc Natl Acad Sci USA 93:6405–6409. https://doi.org/10.1073/pnas.93.13.6405
Cartmill M, Milton K (1977) The lorisiform wrist joint and the evolution of "brachiating" adaptations in the Hominoidea. Am J Phys Anthropol 47:249–272. https://doi.org/10.1002/ajpa.1330470206
Channon AJ, Crompton RH, Günther MM, D'Août K, Vereecke EE (2010) The biomechanics of leaping in gibbons. Am J Phys Anthropol 143:403–416. https://doi.org/10.1002/ajpa.21329
Collyer ML, Adams DC (2022) RRPP: Linear Model Evaluation with Randomized Residuals in a Permutation Procedure, R package version 1.2.3. https://rdocumentation.org/packages/RRPP/versions/1.2.3
Daver G, Nakatsukasa M (2015) *Proconsul heseloni* distal radial and ulnar epiphyses from the Kaswanga Primate Site, Rusinga Island, Kenya. J Hum Evol 80:17–33. https://doi.org/10.1016/j.jhevol.2014.06.021
DeSilva JM, Steininger CM, Patel BA (2013) Cercopithecoid primate postcranial fossils from Cooper's D, South Africa. Geobios 46:381–394. https://doi.org/10.1016/J.GEOBIOS.2013.07.001
Drake RE, Van Couvering JA, Pickford MH, Curtis GH, Harris JA (1988) New chronology for the early Miocene mammalian faunas of Kisingiri, Western Kenya. J Geol Soc Lond 145:479–491. https://doi.org/10.1144/gsjgs.145.3.0479
Drapeau MSM (2008) Articular morphology of the proximal ulna in extant and fossil hominoids and hominins. J Hum Evol 55:86–102. https://doi.org/10.1016/j.jhevol.2008.01.005
Feldesman MR (1982) Morphometric analysis of the distal humerus of some Cenozoic catarrhines: The late divergence hypothesis revisited. Am J Phys Anthropol 59:73–95. https://doi.org/10.1002/ajpa.1330590108
Fleagle JG (1976) Locomotion and posture of the Malayan siamang and implications for hominoid evolution. Folia Primatol 26:245–269. https://doi.org/10.1159/000155756
Fleagle JG (1983) Locomotor adaptations of Oligocene and Miocene hominoids and their phyletic implications. In: Ciochon RL, Corruccini RS (eds) New Interpretations of Ape and Human Ancestry. Plenum Press, New York, pp 301–324. https://doi.org/10.1007/978-1-4684-8854-8_11
Fleagle JG, Simons EL (1982) The humerus of *Aegyptopithecus zeuxis*: a primitive anthropoid. Am J Phys Anthropol 59:175–193. https://doi.org/10.1002/ajpa.1330590207
Gebo DL 1993 Postcranial anatomy and locomotor adaptation in early African anthropoids. In: Gebo DL (ed) Postcranial Adaptation in Nonhuman Primates. Northern Illinois University Press, DeKalb, pp 220–234.
Gilbert CC, Ortiz A, Pugh KD, Campisano CJ, Patel BA, Singh NP, Fleagle JG, Patnaik R (2020a) New middle Miocene ape (Primates: Hylobatidae) from Ramnagar, India fills major gaps in the hominoid fossil record. Proc R Soc B 287:20201655. https://doi.org/10.1098/rspb.2020.1655

Gilbert CC, Pugh KD, Fleagle JG (2020b) Dispersal of Miocene hominoids (and pliopithecoids) from Africa to Eurasia in light of changing tectonics and climate. In: Prasad GV, Patnaik R (eds) Biological Consequences of Plate Tectonics. New Perspectives on Post-Gondwana Break-Up—A Tribute to Ashok Sahni. Springer, Cham, pp 393–412. https://doi.org/10.1007/978-3-030-49753-8_17

Godfrey LR, Sutherland MR, Paine RR, Williams FL, Boy DS, Vuillaume-Randriamanantena M (1995) Limb joint surface areas and their ratios in Malagasy lemurs and other mammals. Am J Phys Anthropol 97:11–36. https://doi.org/10.1002/ajpa.1330970103

Grafen A (1989) The Phylogenetic Regression. Philos Trans R Soc Lond B 326:119–157. https://doi.org/10.1098/rstb.1989.0106

Gunz P, Mitteroecker P, Neubauer S, Weber GW, Bookstein FL 2009 Principles for the virtual reconstruction of hominin crania. J Hum Evol 57:48–62. https://doi.org/10.1016/j.jhevol.2009.04.004

Halenar LB (2011) Reconstructing the locomotor repertoire of *Protopithecus brasiliensis*. II. Forelimb morphology. Anat Rec 294:2048–2063. https://doi.org/10.1002/ar.21499

Harrison T (1987) The phylogenetic relationships of the early catarrhine primates: a review of the current evidence. J Hum Evol 16:41–80. https://doi.org/10.1016/0047-2484(87)90060-1

Harrison T (2005) The zoogeographic and phylogenetic relationships of early catarrhine primates in Asia. Anthropol Sci 113:43–51. https://doi.org/10.1537/ase.04S006

Harrison T (2010) Dendropithecoidea, Proconsuloidea, and Hominoidea (Catarrhini, Primates). In: Werdelin L, Sanders WJ (eds) Cenozoic Mammals of Africa. University of California Press, Berkeley, pp 429–469. https://doi.org/10.1525/california/9780520257214.003.0024

Harrison T (2013) Catarrhine origins. In: Begun DR (ed) A Companion to Paleoanthropology. Blackwell Publishing, Chichester, pp 377–396. https://doi.org/10.1002/9781118332344.ch20

Harrison T (2025) A new look at *Laccopithecus robustus* from the Late Miocene of China: anatomy, systematics, and paleobiology. J Hum Evol 206:103728. https://doi.org/10.1016/j.jhevol.2025.103728

Harrison T, Gu Y (1999) Taxonomy and phylogenetic relationships of early Miocene catarrhines from Sihong, China. J Hum Evol 37:225–277. https://doi.org/10.1006/JHEV.1999.0310

Harrison T, Rein TR (2016) The hands of fossil non-hominoid anthropoids. In: Kivell T, Lemelin P, Richmond B, Schmitt D (eds) The Evolution of the Primate Hand: Perspectives from Anatomical, Developmental, Functional and Paleontological evidence. Springer, New York, pp 455–483. https://doi.org/10.1007/978-1-4939-3646-5_16

Harrison T, Zhang Y, Wei G, Sun C, Wang Y, Liu J, Tong H, Huang B, Xu F (2020) A new genus of pliopithecoid from the late Early Miocene of China and its implications for understanding the paleozoogeography of the Pliopithecoidea. J Hum Evol 145:102838. https://doi.org/10.1016/j.jhevol.2020.102838

Hunt KD, Cant JG, Gebo DL, Rose MD, Walker SE, Youlatos D (1996) Standardized descriptions of primate locomotor and postural modes. Primates 37:363–387. https://doi.org/10.1007/BF02381373

Inouye S (1994) Ontogeny of knuckle-walking hand postures in African apes. J Hum Evol 26:459–485. https://doi.org/10.1006/jhev.1994.1028

Ji X, Harrison T, Zhang Y, Wu Y, Zhang C, Hu J, Wu D, Hou Y, Li S, Wang G, Wang Z (2022) The earliest hylobatid from the Late Miocene of China. J Hum Evol 171:103251. https://doi.org/10.1016/j.jhevol.2022.103251

Johnes AL (2004) The evolution of brachiation in atelines: a phylogenetic comparative study. Dissertation, University of California, Davis

Jouffroy FK, Lessertisseur J (1979) Relationships between limb morphology and locomotor adaptations among prosimians: an osteometric study. In: Morbeck ME, Preuschoft H, Gomberg N (eds) Environment, Behavior, and Morphology: Dynamic Interactions in Primates. Gustav Fischer, New York, pp 143–181

Jungers WL (1979) Locomotion, limb proportions, and skeletal allometry in lemurs and lorises. Folia Primatol 32:8–28. https://doi.org/10.1159/000155901

Kamilar JM, Cooper N (2013) Phylogenetic signal in primate behaviour, ecology and life history. Phil Trans R Soc Lond B 368:20120341 https://doi.org/10.1098/rstb.2012.0341

Kelley J (1997) Paleobiological and phylogenetic significance of life history in Miocene hominoids. In: Begun DR, Ward CV, Rose MD (eds) Function, Phylogeny and Fossils: Miocene Hominoid Evolution and Adaptation. Plenum Press, New York, pp. 173–208.

Kelley J (2002) The hominoid radiation in Asia. In: Hartwig WC (ed) The Primate Fossil Record. Cambridge University Press, Cambridge, pp 369–384

Kivell TL, Schmitt D (2009) Independent evolution of knuckle-walking in African apes shows that humans did not evolve from a knuckle-walking ancestor. Proc Natl Acad Sci U S A 106:14241–14246. https://doi.org/10.1073/pnas.0901280106

Köhler M, Moyà-Solà S, Alba DM (2001) Eurasian hominoid evolution in the light of recent *Dryopithecus* findings. In: de Bonis L, Koufos G, Andrews PA (eds) Hominoid Evolution and Climatic Change in Europe, Vol. 2. Cambridge University Press, Cambridge, pp 193–212. https://doi.org/10.1017/CBO9780511600449.008

Kordos L, Begun DR (1999) Femora of *Anapithecus* from Rudabánya. Am J Phys Anthropol 108(S28):173

Kordos L, Begun DR (2001) Primates from Rudabánya: Allocation of specimens to individuals, sex and age categories. J Hum Evol 40:17–39. https://doi.org/10.1006/jhev.2000.0437

Kuhn M, Johnson K (2013) Measuring performance in regression models. In: Kuhn, M, Johnson, K (eds) Applied Predictive Modeling. Springer, New York, pp 95–100. https://doi.org/10.1007/978-1-4614-6849-3_11

Larson SG(1998) Parallel evolution in the hominoid trunk and forelimb. Evol Anthropol 6:87–99. 10.1002/(SICI)1520 https://doi.org/10.1002/(SICI)1520

Lartet É (1856) Note sur un grand Singe fossile qui se rattache au grouppe des Singes supérieurs. C R Acad Sci Paris 43:219–223

Le Gros Clark WE, Thomas DP (1951) Associated jaws and limb bones of *Limnopithecus macinnesi*. Foss Mamm Afr 3:1–27

Leakey REF, Leakey MG (1987) A new Miocene small-bodied ape from Kenya. J Hum Evol 16:369–387. https://doi.org/10.1016/0047-2484(87)90067-4

Manfreda E, Mitteroecker P, Bookstein FL, Schaefer K 2006 Functional morphology of the first cervical vertebra in humans and nonhuman primates. Anat Rec 289B:184–194. https://doi.org/10.1002/ar.b.20113

McCrossin ML, Benefit BR (1997) On the relationships and adaptations of *Kenyapithecus*, a large-bodied hominoid from the Middle Miocene of Eastern Africa. In: Begun DR, Ward CV, Rose MD (eds) Function, Phylogeny, and Fossils: Miocene Hominoid Evolution and Adaptation. Plenum Press, New York, pp 241–267. https://doi.org/10.1007/978-1-4899-0075-3_12

McCrossin ML, Benefit BR, Gitau SN, Palmer AK, Blue KT (1998) Fossil evidence for the origins of terrestriality among Old World higher primates. In: Strasser E, Fleagle J, Rosenberger A, McHenry H (eds) Primate Locomotion. Recent Advances. Plenum Press, New York, pp 353–396. https://doi.org/10.1007/978-1-4899-0092-0_19

McHenry HM, Corruccini RS (1975) Distal humerus in hominoid evolution. Folia Primatol 23:227–244. https://doi.org/10.1159/000155673

Meldrum DJ, Pan Y (1988) Manual proximal phalanx of *Laccopithecus robustus* from the latest Miocene site of Lufeng. J Hum Evol 17:719–731. https://doi.org/10.1016/0047-2484(88)90062-0

Mittermeier RA (1978) Locomotion and posture in *Ateles geoffroyi* and *Ateles paniscus*. Folia Primatol 30:161–193. https://doi.org/10.1159/000155862

Mittermeier RA, Fleagle JG (1976) The locomotor and postural repertoires of *Ateles geoffroyi* and *Colobus guereza*, and a reevaluation of the locomotor category semibrachiation. Am J Phys Anthropol 45:235–255. https://doi.org/10.1002/ajpa.1330450210

Mitteroecker P, Bookstein F (2011) Linear discrimination, ordination, and the visualization of selection gradients in modern morphometrics. Evol Biol 38:100–114. https://doi.org/10.1007/s11692-011-9109-8

Monclús-Gonzalo O, Alba DM, Duhamel A, Fabre A-C, Marigó J (2023) Early euprimates already had a diverse locomotor repertoire: Evidence from ankle bone morphology. J Hum Evol 181:103395. https://doi.org/10.1016/j.jhevol.2023.103395

Monclús-Gonzalo O, Pal S, Püschel TA, Urciuoli A, Vinuesa V, Robles JM, Almécija S, Alba DM (2025a) A dryopithecine talus from Abocador de Can Mata (Vallès-Penedès Basin, NE Iberian Peninsula): Morphometric affinities and evolutionary implications for hominoid locomotion. Am J Biol Anthropol 186:e70043. https://doi.org/10.1002/ajpa.70043

Monclús-Gonzalo O, Alba DM, Fabre A-C, Marigó J (2025b) Reconstruction of the locomotor repertoire of early primates in the light of astragalar and calcaneal shape. J Hum Evol 206: 103730. https://doi.org/10.1016/j.jhevol.2025.103730

Monroy-Cendales MJ, Vélez-García JF, Castañeda-Herrera FE (2020) Gross anatomy of the shoulder and arm intrinsic muscles in the white-footed tamarin (*Saguinus leucopus* – Günther, 1876): Inter- and intraspecific anatomical variations. J Med Primatol 49:123–135. https://doi.org/10.1111/jmp.12465

Moyà-Solà S, Köhler M (1996) A *Dryopithecus* skeleton and the origins of great-ape locomotion. Nature 379:156–159. https://doi.org/10.1038/379156a0

Moyà-Solà S, Köhler M, Alba DM, Casanovas-Vilar I, Galindo J (2004) *Pierolapithecus catalaunicus*, a new Middle Miocene great ape from Spain. Science 306:1339–1344. https://doi.org/10.1126/science.1103094

Moyà-Solà S, Köhler M, Alba DM, Casanovas-Vilar I, Galindo J (2005) Response to comment on "*Pierolapithecus catalaunicus*, a new Middle Miocene great ape from Spain". Science 308:203d. https://doi.org/10.1126/science.1108433

Nakatsukasa M, Kunimatsu Y (2009) *Nacholapithecus* and its importance for understanding hominoid evolution. Evol Anthropol 18:103–119. https://doi.org/10.1002/evan.20208

Nakatsukasa M, Tsujikawa H, Shimizu D, Takano T, Kunimatsu Y, Nakano Y, Ishida H (2003) Definitive evidence for tail loss in *Nacholapithecus*, an East African Miocene hominoid. J Hum Evol 45:179–186. https://doi.org/10.1016/S0047-2484(03)00092-7

Nakatsukasa M, Ward CV, Walker A, Teaford MF, Kunimatsu Y, Ogihara N (2004) Tail loss in *Proconsul heseloni*. J Hum Evol 46:777–784. https://doi.org/10.1016/j.jhevol.2004.04.005

Nakatsukasa M, Mbua E, Sawada Y, Sakai T, Nakaya H, Yano W, Kunimatsu Y (2010) Earliest colobine skeletons from Nakali, Kenya. Am J Phys Anthropol 143:365–382. https://doi.org/10.1002/ajpa.21327

Napier JR, Davis PR (1959) The fore-limb skeleton and associated remains of *Proconsul africanus*. Foss Mamm Afr 16:1–69.

Napier JR, Napier PH (1967) A Handbook of Living Primates. Academic Press, London.

Nengo I, Tafforeau P, Gilbert CC, Fleagle JG, Miller ER, Feibel C, Fox DL, Feinberg J, Pugh KD, Berruyer C, Mana S, Engle Z, Spoor F (2017) New infant cranium from the African Miocene sheds light on ape evolution. Nature 548:169–174. https://doi.org/10.1038/nature23456

O'Higgins P (2000) The study of morphological variation in the hominid fossil record: biology, landmarks and geometry. J Anat 197:103–120. https://doi.org/10.1046/j.1469-7580.2000.19710103.x

Pallas L, Youlatos D, Kunimatsu Y, Nakatsukasa M (2026) Elbow anatomy of fossil cercopithecids from Nakali, Kenya: Functional anatomy and taxonomy. J Hum Evol 210:103785. https://doi.org/10.1016/j.jhevol.2025.103785

Peppe DJ, McNulty K, Cote SM, Harcourt-Smith WEH, Dunsworth HM, Van Couvering JA (2009) Stratigraphic interpretation of the Kulu Formation (early Miocene, Rusinga Island, Kenya) and its implications for primate evolution. J Hum Evol 56:447–461. https://doi.org/10.1016/j.jhevol.2009.02.006

Perry JMG, Cooke SB, Runestad Connour JA, Burgess ML, Ruff CB (2018) Articular scaling and body mass estimation in platyrrhines and catarrhines: Modern variation and application to fossil anthropoids. J Hum Evol 115:20–35. https://doi.org/10.1016/j.jhevol.2017.10.008

Pilbeam DR, Simons EL (1971) Humerus of *Dryopithecus* from Saint Gaudens, France. Nature 229:406–407. https://doi.org/10.1038/229406a0

Pilbeam DR, Rose MD, Barry JC, Shah SMI (1990) New *Sivapithecus* humeri from Pakistan and the relationship of *Sivapithecus* and *Pongo*. Nature 348:237–239. https://doi.org/10.1038/348237a0

Preuschoft H (1990) Gravity in primates and its relation to body shape and locomotion. In: Jouffroy FK, Stack MH, Niemitz C (eds) Gravity, Posture and Locomotion in Primates. Firenze, Il Sedicesimo, pp 107–127

Pugh KD (2022) Phylogenetic analysis of Middle-Late Miocene apes. J Hum Evol 165:103140. https://doi.org/10.1016/j.jhevol.2021.103140

Püschel TA, Gladman JT, Bobe R, Sellers WI (2017) The evolution of the platyrrhine talus: A comparative analysis of the phenetic affinities of the Miocene platyrrhines with their modern relatives. J Hum Evol 111:179–201. https://doi.org/10.1016/j.jhevol.2017.07.015

Püschel TA, Marcé-Nogué J, Gladman JT, Bobe R, Sellers WI (2018) Inferring locomotor behaviours in Miocene New World monkeys using finite element analysis, geometric morphometrics and machine-learning classification techniques applied to talar morphology. J R Soc Interface 15:20180520. https://doi.org/10.1098/rsif.2018.0520

Püschel TA, Marcé-Nogué J, Gladman J, Patel BA, Almécija S, Sellers WI (2020) Getting its feet on the ground: Elucidating *Paralouatta*'s semi-terrestriality using the virtual morpho-functional toolbox. Front Earth Sci 8:79. https://doi.org/10.3389/feart.2020.00079

R Core Team (2021) R: A language and environment for statistical computing. R Foundation for Statistical Computing, Vienna. https://www.R-project.org

Rafferty KL, Ruff CB (1994) Articular structure and function in *Hylobates*, *Colobus*, and *Papio*. Am J Phys Anthropol 94:395–408. https://doi.org/10.1002/ajpa.1330940308

Raventós-Izard G, Monclús-Gonzalo O, Moyà-Solà S, Alba DM, Arias-Martorell J (2025) Ulnar morphology of *Pliobates cataloniae* (Pliopithecoidea: Crouzeliidae): Insights into catarrhine locomotor diversity and forelimb evolution. J Hum Evol 202:103663. https://doi.org/10.1016/j.jhevol.2025.103663

Rein TR, Harrison T, Zollikofer CPE (2011) Skeletal correlates of quadrupedalism and climbing in the anthropoid forelimb: Implications for inferring locomotion in Miocene catarrhines. J Hum Evol 61:564–574. https://doi.org/10.1016/j.jhevol.2011.07.005

Rein TR, Harvati K, Harrison T (2015) Inferring the use of forelimb suspensory locomotion by extinct primate species via shape exploration of the ulna. J Hum Evol 78:70–79. https://doi.org/10.1016/j.jhevol.2014.08.010

Revell LJ (2022) phytools: Phylogenetic Tools for Comparative Biology (and Other Things). R package version 1.0–3. https://cran.r-project.org/web/packages/phytools/index.html

Richmond BG, Whalen M (2001) Forelimb function, bone curvature and phylogeny of *Sivapithecus*. In: de Bonis L, Koufos GD, Andrews P (eds) Hominoid Evolution and Climatic Change in Europe: Volume 2: Phylogeny of the Neogene Hominoid Primates of Eurasia. Cambridge University Press, Cambridge, pp 326–348. https://doi.org/10.1017/CBO9780511600449.015

Rohlf FJ, Corti M (2000) Use of two-block partial least-squares to study covariation in shape. Syst Biol 49:740–753. https://doi.org/10.1080/106351500750049806

Rose MD (1983) Miocene hominoid postcranial morphology. Monkey-like, ape-like, neither, or both? In: Ciochon RL, Corruccini RS (eds) New Interpretations of Ape and Human Ancestry. Plenum Press, New York, pp 405–417

Rose MD (1988) Another look at the anthropoid elbow. J Hum Evol 17:193–224. https://doi.org/10.1016/0047-2484(88)90054-1

Rose MD (1993a) Functional anatomy of the primate elbow and forearm. In: Gebo D (ed) Postcranial Adaptation in Nonhuman Primates. Northern Illinois University Press, De Kalb, pp 70–95

Rose MD (1993b) Locomotor anatomy of Miocene hominoids. In: Gebo D (ed) Postcranial Adaptation in Nonhuman Primates. Northern Illinois University Press, De Kalb, pp 252–272

Rose MD (1994) Quadrupedalism in some Miocene catarrhines. J Hum Evol 26:387–411. https://doi.org/10.1006/jhev.1994.1025

Rose MD (1997) Functional and phylogenetic features of the forelimb in Miocene hominoids. In: Begun DR, Ward CV, Rose MD (eds) Function, Phylogeny and Fossils: Miocene Hominoid Evolution and Adaptation. Plenum Press, New York, pp 79–100. https://doi.org/10.1007/978-1-4899-0075-3_5

Rose MD, Leakey MG, Leakey REF, Walker AC (1992) Postcranial specimens of *Simiolus enjiessi* and other primitive catarrhines from the early Miocene of Lake Turkana, Kenya. J Hum Evol 22:171–237. https://doi.org/10.1016/S0047-2484(05)80006-5

Rosenberger AL, Strier KB (1989) Adaptive radiation of the ateline primates. J Hum Evol 18:717–750. https://doi.org/10.1016/0047-2484(89)90102-4

Rosenberger AL, Tejedor MF, Cooke SB, Halenar L, Pekkar S (2009) Platyrrhine ecophylogenetics, past and present. In: Garber P, Estrada A, Bicca-Marques JC, Heymann EW, Strier KB (eds) South American Primates: Comparative Perspectives in the Study of Behavior, Ecology and Conservation. Springer, New York, pp 69–113. https://doi.org/10.1007/978-0-387-78705-3_4

Rossie JB, Gutierrez M, Goble E (2012) Fossil forelimbs of *Simiolus* from Moruorot, Kenya. Am J Phys Anthropol 147(S54):252

Ruff CB (2002) Long bone articular and diaphyseal structure in Old World monkeys and apes, I: Locomotor effects. Am J Phys Anthropol 119:305–342. https://doi.org/10.1002/ajpa.10117

Ruff CB, Runestad JA (1992) Primate limb bone structural adaptations. Annu Rev Anthropol 21:407–433. https://doi.org/10.1146/annurev.an.21.100192.002203

Ruff CB, Harper CM, Goldstein DM, Daegling DJ, McGraw WS (2019) Long bone structural proportions and locomotor behavior in Cercopithecidae. J Hum Evol 132:47–60. https://doi.org/10.1016/j.jhevol.2019.04.003

Russo GA (2016) Comparative sacral morphology and the reconstructed tail lengths of five extinct primates: *Proconsul heseloni*, *Epipliopithecus vindobonensis*, *Archaeolemur edwardsi*, *Megaladapis grandidieri*, and *Palaeopropithecus kelyus*. J Hum Evol 90:135–162. https://doi.org/10.1016/j.jhevol.2015.10.007

Sarmiento EE (1995) Cautious climbing and folivory: A model of hominoid differentiation. Hum Evol 10:289–321. https://doi.org/10.1007/BF02438967

Schlager S, Jefferis G, Dryden I (2022) Morpho: Calculations and Visualisations Related to Geometric Morphometrics. R package version 2.10. https://cran.r-project.org/web/packages/Morpho/Morpho.pdf

Schmitt D, Zeininger A, Granatosky MC (2016) Patterns, variability, and flexibility of hand posture during locomotion in primates. In: Kivell TL, Lemelin P, Richmond BG, Schmitt D (eds.) The Evolution of the Primate Hand: Anatomical, Developmental, Functional, and Paleontological Evidence. Springer, New York, pp 345–369. https://doi.org/10.1007/978-1-4939-3646-5_13

Seiffert ER (2006) Revised age estimates for the later Paleogene mammal faunas of Egypt and Oman. Proc Natl Acad Sci USA 103:5000–5005. https://doi.org/10.1073/pnas.0600689103

Senut B (1986) Long bones of the primate upper limb: Monomorphic or dimorphic? Hum Evol 1:7–22. https://doi.org/10.1007/BF02437282

Senut B (1989) Le Coude des Primates Hominoïdes. Anatomie, Fonction, Taxonomie, Évolution. Éditions du Centre National de la Recerche Scientifique, Paris

Senut B (2012) Les restes post-crâniens des Pliopithecidae (Primates) de Sansan. Mém Mus Hist Nat Paris 203:535–558

Simons E (1995) Egyptian Oligocene primates: a review. Am J Phys Anthropol 38:199–238. https://doi.org/10.1002/ajpa.1330380610

Stern JT Jr, Larson SG (2001) Telemetered electromyography of the supinators and pronators of the forearm in gibbons and chimpanzees: implications for the fundamental positional adaptation of hominoids. Am J Phys Anthropol 115:253–268. https://doi.org/10.1002/ajpa.1080

Su DF, Jablonski NG (2009) Locomotor behavior and skeletal morphology of the odd-nosed monkeys. Folia Primatol 80:189–219. https://doi.org/10.1159/000240967

Symonds MRE, Blomberg SP (2014) A primer on phylogenetic generalised least squares. In: Garamszegi L (eds) Modern Phylogenetic Comparative Methods and Their Application in Evolutionary Biology. Springer, Berlin, pp 105–130. https://doi.org/10.1007/978-3-662-43550-2_5

Szalay FS, Dagosto M (1980) Locomotor adaptations as reflected on the humerus of Paleogene primates. Folia Primatol 34:1–45. https://doi.org/10.1159/000155946

Szalay FS, Delson E (1979) Evolutionary History of the Primates. Academic Press, New York. https://doi.org/10.1016/C2009-0-22035-6

Takano T, Nakatsukasa M, Kunimatsu Y, Nakano Y, Ogihara N, Ishida H (2018) Forelimb long bones of *Nacholapithecus* (KNM-BG 35250) from the middle Miocene in Nachola, northern Kenya. Anthropol Sci 126:135–149. https://doi.org/10.1537/ase.181022

Tallman M, Cooke SB (2016) New endemic platyrrhine humerus from Haiti and the evolution of the Greater Antillean platyrrhines. J Hum Evol 91:144–166. https://doi.org/10.1016/j.jhevol.2015.10.010

Urciuoli A, Alba DM (2023) Systematics of Miocene apes: State of the art of a neverending controversy. J Hum Evol 175:103309. https://doi.org/10.1016/j.jhevol.2022.103309

Urciuoli A, Zanolli C, Beaudet A, Pina M, Almécija S, Moyà-Solà S, Alba DM (2021) A comparative analysis of the vestibular apparatus in *Epipliopithecus vindobonensis*: Phylogenetic implications. J Hum Evol 151:102930. https://doi.org/10.1016/j.jhevol.2020.102930

Urciuoli A, Zanolli C, Bouchet F, Arias-Martorell J, Costeur L, Rook L, Alba DM (2026) New evidence from the bony labyrinth and teeth of the Late Miocene ape *Oreopithecus* based on a partial cranium from Baccinello. J Mamm Evol 33:6. https://doi.org/10.1007/s10914-025-09793-0

van der Meulen AJ, García-Paredes I, Álvarez-Sierra MA, van den Hoek Ostende LW, Hordijk K, Oliver A, López-Guerrero P, Hernández-Ballarín V, Peláez-Campomanes P (2011) Biostratigraphy or biochronology? Lessons from the Early and Middle Miocene small mammal events in Europe. Geobios 44:309–321. https://doi.org/10.1016/j.geobios.2010.11.004

Vanhoof MJM, van Leeuwen T, Vereecke EE (2020) The forearm and hand musculature of semi-terrestrial rhesus macaques (*Macaca mulatta*) and arboreal gibbons (Fam. Hylobatidae). Part I. Description and comparison of the muscle configuration. J Anat 237:774–790. https://doi.org/10.1111/joa.13222

Vanhoof MJM, van Leeuwen T, Galletta L, Vereecke EE (2021) The forearm and hand musculature of semi-terrestrial rhesus macaques (*Macaca mulatta*) and arboreal gibbons (fam. Hylobatidae). Part II. Quantitative analysis. J Anat 238:321–337. https://doi.org/10.1111/joa.13314

Walker A (1974) Locomotor adaptations in past and present prosimian primates. In: Jenkins FA (ed) Primate Locomotion. Academic Press, New York, pp 349–381. https://doi.org/10.1016/B978-0-12-384050-9.50016-7

Walker A (1997) *Proconsul*. Function and phylogeny. In: Begun DR, Ward CV, Rose MD (eds) Function, Phylogeny, and Fossils: Miocene Hominoid Evolution and Adaptations. Plenum Press, New York, pp 209–224. https://doi.org/10.1007/978-1-4899-0075-3_10

Ward CV (1993) Torso morphology and locomotion in *Proconsul nyanzae*. Am J Phys Anthropol 92:291–328. https://doi.org/10.1002/ajpa.1330920306

Ward CV (1998) *Afropithecus*, *Proconsul*, and the primitive hominoid skeleton. In: Strasser E, Fleagle JG, Rosenberg AL, McHenry HM (eds) Primate Locomotion: Recent Advances. Plenum Press, New York, pp 337–352. https://doi.org/10.1007/978-1-4899-0092-0_18

Ward CV (2015) Postcranial and locomotor adaptations of hominoids. In: Henke W, Tattersall I (eds) Handbook of Paleoanthropology, 2nd ed. Springer, Heidelberg, pp 1363–1386. https://doi.org/10.1007/978-3-642-39979-4_34

Ward CV, Walker A, Teaford MF (1991) *Proconsul* did not have a tail. J Hum Evol 21:215–220. https://doi.org/10.1016/0047-2484(91)90062-Z

Willmott, CJ, Matsuura K (2005) Advantages of the mean absolute error (MAE) over the root mean square error (RMSE) in assessing average model performance. Clim Res 30:79–82. https://doi.org/10.3354/cr030079

Wold S, Sjöström M, Eriksson L (2001) PLS-regression: A basic tool of chemometrics. Chemometr Intell Lab Syst 58:109–130. https://doi.org/10.1016/S0169-7439(01)00155-1

Youlatos D, Couette S, Halenar LB (2015) Morphology of howler monkeys: A review and quantitative analyses. In: Kowalewski MM, Garber PA, Cortés-Ortiz L, Urbani B, Youlatos D (eds) Howler Monkeys. Adaptive Radiation, Systematics, and Morphology. Springer, New York, pp 133–176. https://doi.org/10.1007/978-1-4939-1957-4_6

Zapfe H (1958) The skeleton of *Pliopithecus* (*Epipliopithecus*) *vindobonensis* Zapfe and Hürzeler. Am J Phys Anthropol 16:441–457. https://doi.org/10.1002/ajpa.1330160405

Zapfe H (1961) Die Primatenfunde aus der miozänen Spaltenfüllung von Neudorf an der March (Děvínská Nová Ves), Tschechoslowakei. Schweiz Palaeontol Abh 78:1–293

Zapfe H, Hürzeler J (1957) Die Fauna der mioziinen Spaltenfullung von Neudorf an der March (ČSR). Primates. Sber Österr Akad Wiss Mathem-nat Kl 166:113–123

Zelazny KG (2019) Morphological variation in the distal humerus of extant hominids and fossil hominins. Doctoral dissertation, The Johns Hopkins University, Baltimore

Zelditch ML, Swiderski DL, Sheets HD, Fink WL (2012) Geometric Morphometrics for Biologists: A Primer. Elsevier Academic Press, New York. https://doi.org/10.1016/B978-0-12-778460-1.X5000-5